Relay Assisted Physical Resource Sharing: Projection Based Separation of Multiple Operators (ProBaSeMO) for Two-Way Relaying With MIMO Amplify and Forward Relays

Jianshu Zhang, *Student Member, IEEE*, Florian Roemer, *Student Member, IEEE*, and Martin Haardt, *Senior Member, IEEE*

***Abstract*—In this paper, we investigate a relay-assisted resource sharing scenario, namely, multi-operator two-way relaying with a MIMO amplify-and-forward (AF) relay. Here, the spectrum and the relay (infrastructure) are shared among multiple operators. We develop the projection based separation of multiple operators (ProBaSeMo) relay transmit strategy, which is inspired by the block diagonalization (BD) and regularized block diagonalization (RBD) schemes that are space-division multiple access (SDMA) approaches for multi-user MIMO systems. If the user terminals are equipped with multiple antennas, appropriate precoding and decoding matrix designs are also proposed. Compared to the time-shared approach where the relay is used by different operators in a time division multiple access (TDMA) manner, we demonstrate that the ProBaSeMO algorithms can provide a significant sharing gain in terms of the sum rate with many antennas at the relay or in the high SNR regime in a two-operator case. For a fixed number of antennas at the relay, an even higher sharing gain can be obtained if the number of operators increases.**

***Index Terms*—Amplify and forward relay, MIMO, physical resource sharing, two-way relaying.**

I. Introduction

In general, the physical resources in communications engineering are spectrum and infrastructure [6]. Traditionally these resources are allocated orthogonally or exclusively in frequency, time, space inside the network of a single operator or among the networks of different operators. Nevertheless, it is shown in [9] that spectrum sharing offers the potential to improve the network spectral efficiency. It is also reported that infrastructure (including network equipments, sites, etc.) sharing provides advantages like reduced capital expenditures and operating expenditures [1]. However, by sharing physical resources, new types of interference are created on the physical layer. Handling these new types of interference poses a significant and novel challenge to the design of appropriate transmission techniques.

In this paper, we present a relay-assisted resource sharing scenario in which multiple communication partners (belonging to different operators) use one relay (possibly owned by a third party/virtual operator) to bidirectionally exchange information using the same spectrum. The relay has multiple antennas and operates in a half-duplex mode. Note that this scenario includes spectrum as well as infrastructure (relay) sharing and has attractive practical applications. One concrete application for this kind of relay sharing is the metropolitan scenario as shown in Fig. 1. Here, strong shadowing effects may cause many coverage holes. Therefore, dense networks are required to guarantee the quality of service (QoS) at the user terminals (UTs). Also taking into account that more than one operators or service providers operate in the same area, if they share the relays as well as the spectrum, this leads to lower capital expenditures and operating expenditures for all the operators. Another application is a disaster scenario where the base station cannot provide services any more. Then the relays can be deployed to temporarily maintain the communication among the local residents. Concerning the privacy and the competitiveness of different operators, in our scenario amplify and forward (AF) relays are preferable since they avoid complex signaling and data sharing among operators, e.g., an AF relay does not need the knowledge of the modulation and coding formats of different operators as opposed to the regenerative relaying strategies such as decode-and-forward. Moreover, AF relays significantly reduce the delay and the complexity.

One-way relaying techniques with MIMO AF relays have been well studied. For example, the optimal beamforming design for single pair one-way relaying systems with single-antenna or multiple-antenna UTs are studied in [5] and [8], respectively. In [3] it is also implicitly shown that sharing relays between multiple UT pairs outperforms the TDMA scheme. Nevertheless, two-way relaying (TWR) can compensate the spectral efficiency loss of one-way relaying due to the half-duplex constraint and therefore uses the radio resources more efficiently [13]. Previous work on TWR systems with MIMO AF relays

Manuscript received April 29, 2011; revised December 08, 2011 and April 13, 2012; accepted May 05, 2012. Date of publication May 23, 2012; date of current version August 07, 2012. The associate editor coordinating the review of this manuscript and approving it for publication was Prof. Yimin D. Zhang. This work was performed in the framework of the European research project SAPHYRE, which is partly funded by the European Union under its FP7 ICT Objective 1.1—The Network of the Future. The material in this paper was presented in part at the Future Network and Mobile Summit, Florence, Italy, June 2010.

The authors are with the Ilmenau University of Technology, Communications Research Laboratory, D-98684 Ilmenau, Germany (e-mail: Jianshu.Zhang@tu-ilmenau.de; Florian.Roemer@tu-ilmenau.de; Martin.Haardt@tu-ilmenau.de).

Color versions of one or more of the figures in this paper are available online at http://ieeexplore.ieee.org.

Digital Object Identifier 10.1109/TSP.2012.2200888

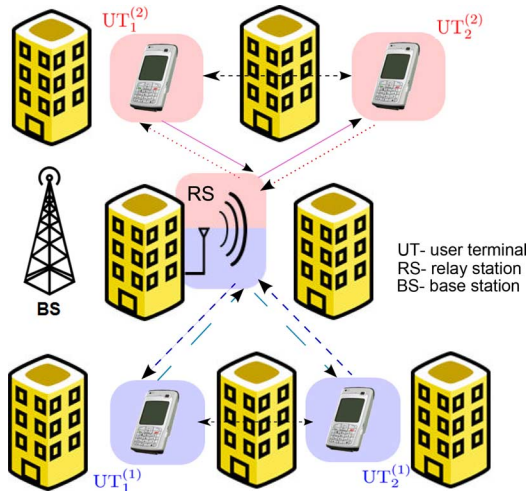

Fig. 1. A typical metropolitan scenario. The arrows show the data flow in two phases, i.e., in the first time slot, all the UTs transmit to the relay and the relay amplifies and sends the signal to all the UTs in the second time slot.

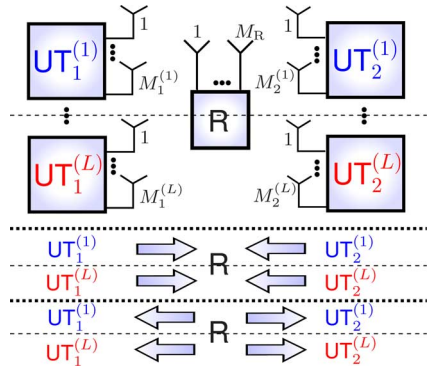

Fig. 2. Multi-operator two-way relaying system model. The kth terminal belonging to the ℓth operator has $M_k^{(\ell)}$ antennas and the relay station is equipped with M_R antennas.

includes [7], [10], [14], [15], [21], [22]. The optimal beamforming technique [10], [22], as well as several linear preprocessing techniques [14], [15], have been proposed for the single pair two-way AF relay channel. Beamforming solutions for the multi-pair two-way MIMO relay channel are shown in [7], [21]. The transmit strategy proposed in [7] is based on zero-forcing (ZF) and minimum mean-square-error (MMSE) criteria. In [21] the authors consider single antenna UTs and focus on the quantize and forward relaying strategy. However, to our knowledge, no references deal with the relay sharing scenario other than our previous work in [17]. Therefore, we consider the transmit strategy design to accomplish this form of spectrum and infrastructure sharing by exploiting the multiple antennas at the relay.

A traditional transmit strategy for our scenario is to assign the physical resources to all the operators in an orthogonal manner, e.g., via different time slots (TDMA manner which is the time-shared approach used in this paper). Hence, if there is voluntary infrastructure (relay) and spectrum sharing, three important questions arise:

- What are the potential gains (losses) with respect to the chosen performance metric (e.g., the system sum rate, the achievable rate region, etc.) as compared to the orthogonally sharing (e.g., time-shared) approach?
- What are the parameter settings such that a significant gain is achieved?
- What is the order of magnitude of the gain?

These are the questions that we will answer in this paper. In the following, we will focus on the system model shown in Fig. 2. A multi-antenna AF relay is deployed to assist the communication between pairs of UTs belonging to different operators. This system model has the same mathematical formulation as the multi-pair TWR scenario with a MIMO AF relay. Thereby, each UT experiences not only the intra-operator interference (the self-interference (SI) caused by its own transmitted signal) but also the inter-operator interference (interference caused by other data signals dedicated to the UTs of other operators). The SI can be subtracted at the UTs if channel knowledge can be acquired. Depending on whether to subtract the SI at the UTs, the spatial division multiple access (SDMA) based techniques for our scenario can be categorized into pairing aware methods (in which the SI is subtracted at the UTs), e.g., [17], [21]) and non-pairing aware methods (in which the SI is nulled at the relay, e.g., [7]).

In this paper, we propose a pairing aware relay transmit strategy which is the projection based separation of multiple operators (ProBaSeMO). Using ProBaSeMO, the system is firstly decoupled into multiple independent single-operator TWR subsystems via inter-operator interference suppression techniques at the relay. Then, arbitrary transmit strategies for single-operator two-way AF MIMO relaying are applied to enhance the performance of the subsystems of each operator. In this work we choose the algebraic norm-maximizing (ANOMAX) algorithm [14] and the rank-restored ANOMAX (RR-ANOMAX) algorithm [15] as the single-operator strategies. Note that the ProBaSeMO approach also exploits MIMO techniques at the UTs. Thus it is more general compared to the work in [21]. Next, to get a benchmark for the ProBaSeMO strategy, we study the sum rate maximization problem subject to a transmit power constraint at the relay. The original problem is non-convex. Nonetheless, for the single-antenna UT case, the global optimum is achieved using the power method. For the multiple-antenna UT case, we apply the steepest descent method. However, both methods require many iterations and thus their computational complexity is much higher compared to the ProBaSeMO approach. Afterwards, we introduce a least square (LS) based channel estimation algorithm for acquiring channel knowledge at both the relay and each UT. The performance comparison in terms of the system sum rate, the system BER and the average spectral efficiency is shown. Simulation results demonstrate that i) Compared to the time-shared approach, the ProBaSeMO approach can achieve a significant sharing gain with many antennas at the relay or in the high SNR regime regardless of single stream transmission or multiple stream transmission at the UTs. For a fixed number of antennas at the relay, a higher sharing gain can be obtained if the number of operators which share the relay increases. The sharing gain in this paper is defined as the performance comparison of the non-orthogonal sharing approaches and the time-shared approach in terms of system sum rate. ii) compared to the

non-pairing aware approach in [7], the ProBaSeMO approach has a better sum rate performance especially in the high SNR regime and is more robust to the spatial correlation at the relay. iii) the ProBaSeMO scheme has almost the same performance as the optimum solution for the single-antenna case and suffers only a little loss compared to the steepest descent method for the multiple-antenna case.

The rest of the paper is organized as follows. In Section II, the data model is introduced. In Section III, the proposed ProBaSeMO approach as well as the design of transmit strategies at the UTs are presented. The sum rate maximization problem is discussed in Section IV. Section V illustrates a proposed channel estimation scheme for this system. In Section VI simulation results are shown. A short summary follows in Section VII. Some detailed derivations are found in the Appendix.

Notation: Upper-case and lower-case bold-faced letters denote matrices and vectors, respectively. The expectation, trace of a matrix, transpose, conjugate, Hermitian transpose, and Moore-Penrose pseudo inverse are denoted by $\mathbb{E}\{\cdot\}$, $\mathrm{Tr}\{\cdot\}$, $\{\cdot\}^{\mathrm{T}}$, $\{\cdot\}^{*}$, $\{\cdot\}^{\mathrm{H}}$, and $\{\cdot\}^{+}$, respectively. The m-by-m identity matrix is $\boldsymbol{I}_m$. The m-by-n matrix with all zero elements is $\boldsymbol{0}_{m\times n}$. The Euclidean norm of a vector and the Frobenius norm of a matrix are denoted by $\|\cdot\|$ and $\|\cdot\|_{\mathrm{F}}$, respectively. The operator $|\cdot|$ denotes the absolute value or the determinant of a matrix. The Kronecker product is $\otimes$. The $\mathrm{vec}\{\cdot\}$ operator stacks the columns of a matrix into a vector. The $\mathrm{unvec}_{m\times n}\{\cdot\}$ operator stands for the inverse function of $\mathrm{vec}\{\cdot\}$. The operator $\mathrm{diag}\{\boldsymbol{v}\}$ creates a diagonal matrix by aligning the elements of the vector $\boldsymbol{v}$ onto its diagonal and $\mathrm{blkdiag}\{\cdot\}$ creates a block diagonal matrix. The rank of a matrix is denoted by $\mathrm{rank}\{\cdot\}$.

II. Data Model

The scenario under investigation is shown in Fig. 2. Pairs of UTs belonging to L different operators want to communicate with each other. However, due to the poor quality of the direct channel between these pairs of UTs, they can communicate only with the help of the relay. For notational simplicity, the kth UT of the ℓth operator has $M_k^{(\ell)} = M_{\mathrm{U}}$ antennas $\forall k,\ell$ ($k \in \{1,2\}$ is the UT index, $\ell \in \{1,\ldots,L\}$ denotes the operator index). The relay is equipped with M_{R} antennas. We assume that the synchronization is perfect[1] and the channel is flat fading. The channel between the kth UT of the ℓth operator and the relay is denoted by $\boldsymbol{H}_k^{(\ell)} \in \mathbb{C}^{M_{\mathrm{R}}\times M_{\mathrm{U}}}$. Furthermore, we assume $\boldsymbol{H}_k^{(\ell)}$ is a full rank matrix which implies $\mathrm{rank}\{\boldsymbol{H}_k^{(\ell)}\} = \min\{M_{\mathrm{R}}, M_{\mathrm{U}}\}$.

The two-way AF relaying protocol consists of two transmission phases: in the first phase, which could also be called MAC (Multiple Access) phase, all the UTs transmit their data simultaneously to the relay. Let the kth UT of the ℓth operator transmit the data vector $\boldsymbol{s}_k^{(\ell)} \in \mathbb{C}^{r_k^{(\ell)}}$ with transmit precoding matrix $\boldsymbol{W}_k^{(\ell)} \in \mathbb{C}^{M_{\mathrm{U}}\times r_k^{(\ell)}}$ ($r_k^{(\ell)}$ is the number of transmitted data streams of the corresponding UT.). Then its transmitted signal vector $\boldsymbol{x}_k^{(\ell)}$ can be written as

$$\boldsymbol{x}_k^{(\ell)} = \boldsymbol{W}_k^{(\ell)}\boldsymbol{s}_k^{(\ell)}, \tag{1}$$

with the transmit power constraint $\mathbb{E}\left\{\|\boldsymbol{x}_k^{(\ell)}\|^2\right\} \le P_k^{(\ell)}$. The elements of the input data vectors $\boldsymbol{s}_k^{(\ell)}$ are independently distributed with zero mean and unit variance.

The received signal vector at the relay is then

$$\boldsymbol{r} = \sum_{\ell=1}^{L}\sum_{k=1}^{2}\boldsymbol{H}_k^{(\ell)}\boldsymbol{x}_k^{(\ell)} + \boldsymbol{n}_{\mathrm{R}} \in \mathbb{C}^{M_{\mathrm{R}}}, \tag{2}$$

where $\boldsymbol{n}_{\mathrm{R}} \in \mathbb{C}^{M_{\mathrm{R}}}$ denotes the zero-mean circularly symmetric complex Gaussian (ZMCSCG) noise vector and $\mathbb{E}\{\boldsymbol{n}_{\mathrm{R}}\boldsymbol{n}_{\mathrm{R}}^{\mathrm{H}}\} = \sigma_{\mathrm{R}}^2\boldsymbol{I}_{M_{\mathrm{R}}}$.

In the second phase, which could also be called BC (Broadcast) phase, the relay amplifies the received signal and then forwards it to all the UTs simultaneously. The signal transmitted by the relay can be expressed as

$$\bar{\boldsymbol{r}} = \boldsymbol{G}\cdot\boldsymbol{r}. \tag{3}$$

where $\boldsymbol{G} \in \mathbb{C}^{M_{\mathrm{R}}\times M_{\mathrm{R}}}$ is the relay amplification matrix. The transmit power constraint at the relay should be fulfilled such that $\mathbb{E}\{\|\bar{\boldsymbol{r}}\|^2\} \le P_{\mathrm{R}}$, where P_{R} denotes the total power at the relay. For notational simplicity, we assume that the reciprocity assumption between the first- and second-phase channels is valid. This assumption is fulfilled in a TDD system if the RF chains are calibrated.[2] The received signal vector $\boldsymbol{y}_k^{(\ell)}$ at the kth UT of the ℓth operator can be written as

$$\begin{aligned}\boldsymbol{y}_k^{(\ell)} &= \boldsymbol{H}_k^{(\ell)^{\mathrm{T}}}\bar{\boldsymbol{r}} + \boldsymbol{n}_k^{(\ell)}\\ &= \underbrace{\boldsymbol{H}_k^{(\ell)^{\mathrm{T}}}\boldsymbol{G}\boldsymbol{H}_{3-k}^{(\ell)}\boldsymbol{x}_{3-k}^{(\ell)}}_{\text{desired signal}} + \underbrace{\boldsymbol{H}_k^{(\ell)^{\mathrm{T}}}\boldsymbol{G}\boldsymbol{H}_k^{(\ell)}\boldsymbol{x}_k^{(\ell)}}_{\text{self-interference}}\\ &\quad + \underbrace{\sum_{\substack{\bar{k}=1,2\\ \bar{\ell}\neq\ell}}\boldsymbol{H}_k^{(\ell)^{\mathrm{T}}}\boldsymbol{G}\boldsymbol{H}_{\bar{k}}^{(\bar{\ell})}\boldsymbol{x}_{\bar{k}}^{(\bar{\ell})}}_{\text{inter-operator interference}}\\ &\quad + \underbrace{\boldsymbol{H}_k^{(\ell)^{\mathrm{T}}}\boldsymbol{G}\boldsymbol{n}_{\mathrm{R}} + \boldsymbol{n}_k^{(\ell)}}_{\text{effective noise}} \in \mathbb{C}^{M_{\mathrm{U}}},\end{aligned} \tag{4}$$

where $\boldsymbol{n}_k^{(\ell)} \in \mathbb{C}^{M_{\mathrm{U}}}$ denotes the ZMCSCG noise vector and $\mathbb{E}\{\boldsymbol{n}_k^{(\ell)}\boldsymbol{n}_k^{(\ell)^{\mathrm{H}}}\} = {\sigma_k^{(\ell)}}^2\boldsymbol{I}_{M_{\mathrm{U}}}$. Then the decoding matrix $\boldsymbol{F}_k^{(\ell)} \in \mathbb{C}^{\bar{r}_k^{(\ell)}\times M_{\mathrm{U}}}$ ($\bar{r}_k^{(\ell)}$ is the number of received data streams of the corresponding UT.) will be used to convert the received signal $\boldsymbol{y}_k^{(\ell)}$ into an estimate of the transmitted data

$$\hat{\boldsymbol{s}}_k^{(\ell)} = \boldsymbol{F}_k^{(\ell)}\boldsymbol{y}_k^{(\ell)}. \tag{5}$$

The overall sum rate of the system is equal to

$$R_{\mathrm{sum}} = \frac{1}{2}\sum_{\ell=1}^{L}\sum_{k=1}^{2}\sum_{i=1}^{\bar{r}_k^{(\ell)}}\log_2(1+\eta_{k,i}^{(\ell)}) \tag{6}$$

[1] In practice, the level of synchronization between UTs of the same operator and UTs of different operators might be different which will have practical impacts on the performance of the proposed algorithms. However, analyzing this issue is out of the scope of this paper since it requires detailed mathematical modeling and analysis.

[2] Our method is not limited to the reciprocity assumption.

where $\eta_{k,i}^{(\ell)}$ is the SINR per stream at each UT and the factor 1/2 is due to the two transmission phases (half duplex). The optimization problem to find the optimal relay amplification matrix as well as the transmit precoding matrix which maximizes (6) subject to a transmit power constrain at the relay is non-convex.

In our work one successful communication consists of a training phase and a data transmission phase. That is, in the first phase each UT only transmits training symbols. These training symbols are used for channel estimation as well as the calculation of the $\boldsymbol{G}$ matrix at the relay. They are also used for channel estimation and the calculation of precoding matrices at the UTs. The algorithms proposed in Sections III and IV are all executed in the training phase. In the data transmission phase, each UT transmits data symbols using the precoding matrices computed from the training phase and the scaled version of the relay amplification matrix $\boldsymbol{G}$ is applied at the relay.[3]

III. Projection Based Separation of Multiple Operators (ProBaSeMO)

The system in Fig. 2 is an interference limited system since the UTs of one operator suffer from both the inter-operator interference which is created by the UTs of the other operators and the additional self-interference which is due to the two-way relaying protocol. We need to manage these interference in an efficient way such that the QoSs of all the UTs can be guaranteed. A similar situation occurs in the multi-user MIMO (MU-MIMO) downlink system. There linear precoding techniques like block diagonalization (BD) [19] and regularized block diagonalization (RBD) [20] first suppress the inter-user interference and then calculate the precoder for each user separately, which simplifies the system design and significantly improves the system performance. Inspired by this two-step strategy for MU-MIMO systems, we propose to first suppress the inter-operator interference in our system, e.g., by designing the relay amplification matrix such that the UTs of one operator transmit and receive in the null space of the combined channels of all the other UTs. Thereby, the system will be decoupled into L parallel independent single-operator TWR subsystems. Then, in the second step, arbitrary transmission techniques for single-operator TWR system can be applied separately on each subsystem. This also facilitates the differentiation among multiple operators. To fulfill the requirement of our proposed projection based separation of multiple operators (ProBaSeMO) approach, we decompose the relay amplification matrix $\boldsymbol{G}$ into

$$\boldsymbol{G} = \gamma_0 \cdot \boldsymbol{G}_0 = \gamma_0 \cdot \boldsymbol{G}_{\mathrm{T}} \cdot \boldsymbol{G}_{\mathrm{S}} \cdot \boldsymbol{G}_{\mathrm{R}} \in \mathbb{C}^{M_{\mathrm{R}} \times M_{\mathrm{R}}} \tag{7}$$

where $\boldsymbol{G}_{\mathrm{R}} \in \mathbb{C}^{LM_{\mathrm{R}} \times M_{\mathrm{R}}}$ and $\boldsymbol{G}_{\mathrm{T}} \in \mathbb{C}^{M_{\mathrm{R}} \times LM_{\mathrm{R}}}$ are filters designed to suppress the inter-operator interference during the MAC phase and BC phase, respectively. The parameter $\gamma_0 \in \mathbb{R}^+$ is chosen such that the transmit power constraint at the relay is fulfilled. Moreover, the dimensions of the system increase such that the block diagonal matrix $\boldsymbol{G}_{\mathrm{S}} \in \mathbb{C}^{LM_{\mathrm{R}} \times LM_{\mathrm{R}}}$ can be written as

$$\boldsymbol{G}_{\mathrm{S}} = \begin{bmatrix} \boldsymbol{G}_{\mathrm{S}}^{(1)} & \cdots & \boldsymbol{0}_{M_{\mathrm{R}} \times M_{\mathrm{R}}} \\ \vdots & \ddots & \vdots \\ \boldsymbol{0}_{M_{\mathrm{R}} \times M_{\mathrm{R}}} & \cdots & \boldsymbol{G}_{\mathrm{S}}^{(L)} \end{bmatrix}, \tag{8}$$

where $\boldsymbol{G}_{\mathrm{S}}^{(1)}, \ldots, \boldsymbol{G}_{\mathrm{S}}^{(L)} \in \mathbb{C}^{M_{\mathrm{R}} \times M_{\mathrm{R}}}$ are the relay amplification matrices for each subsystem. Note that $\boldsymbol{G}_{\mathrm{S}}$ is block diagonal since it represents the processing performed in the individual subsystems.

The overall transmit and receive filter matrices $\boldsymbol{G}_{\mathrm{T}}$ and $\boldsymbol{G}_{\mathrm{R}}$ can also be partitioned as

$$\boldsymbol{G}_{\mathrm{T}} = \left[\boldsymbol{G}_{\mathrm{T}}^{(1)}, \ldots, \boldsymbol{G}_{\mathrm{T}}^{(L)}\right], \quad \boldsymbol{G}_{\mathrm{R}} = \left[\boldsymbol{G}_{\mathrm{R}}^{(1)^{\mathrm{T}}}, \ldots, \boldsymbol{G}_{\mathrm{R}}^{(L)^{\mathrm{T}}}\right]^{\mathrm{T}} \tag{9}$$

where $\boldsymbol{G}_{\mathrm{T}}^{(\ell)} \in \mathbb{C}^{M_{\mathrm{R}} \times M_{\mathrm{R}}}$ and $\boldsymbol{G}_{\mathrm{R}}^{(\ell)} \in \mathbb{C}^{M_{\mathrm{R}} \times M_{\mathrm{R}}}$. In the following we show how to calculate the matrices $\boldsymbol{G}_{\mathrm{T}}^{(\ell)}$, $\boldsymbol{G}_{\mathrm{S}}^{(\ell)}$, and $\boldsymbol{G}_{\mathrm{R}}^{(\ell)}$ for each operator.

A. Block-Diagonalization at the Relay

As mentioned before, to eliminate only the inter-operator interference but leave the intra-operator interference to the UTs themselves, one choice is to adapt the BD technique for MU-MIMO systems in [19] to design the matrices $\boldsymbol{G}_{\mathrm{T}}^{(\ell)}$ and $\boldsymbol{G}_{\mathrm{R}}^{(\ell)}$.

Taking the design of the $\boldsymbol{G}_{\mathrm{R}}^{(\ell)}$ matrix for the MAC phase as an example, let us define the combined channel matrix $\tilde{\boldsymbol{H}}^{(\ell)} \in \mathbb{C}^{M_{\mathrm{R}} \times 2(L-1)M_{\mathrm{U}}}$ for all UTs except the UTs of the ℓth operator as

$$\tilde{\boldsymbol{H}}^{(\ell)} = \left[\boldsymbol{H}^{(1)} \ldots \boldsymbol{H}^{(\ell-1)} \boldsymbol{H}^{(\ell+1)} \ldots \boldsymbol{H}^{(L)}\right], \tag{10}$$

where $\boldsymbol{H}^{(\ell)} = [\,\boldsymbol{H}_1^{(\ell)} \quad \boldsymbol{H}_2^{(\ell)}\,] \in \mathbb{C}^{M_{\mathrm{R}} \times 2M_{\mathrm{U}}}$ is the concatenated channel matrix of the UTs of the ℓth operator. Then the receive filter matrix $\boldsymbol{G}_{\mathrm{R}}^{(\ell)}$ should lie in the left null space of $\tilde{\boldsymbol{H}}^{(\ell)}$ so that the signal of the ℓth operator will not cause interference to all the other operators. Let $\tilde{L}^{(\ell)} = \mathrm{rank}\{\tilde{\boldsymbol{H}}^{(\ell)}\}$ and define the singular value decomposition (SVD) of $\tilde{\boldsymbol{H}}^{(\ell)}$ as

$$\tilde{\boldsymbol{H}}^{(\ell)} = [\,\tilde{\boldsymbol{U}}_{\mathrm{s}}^{(\ell)} \quad \tilde{\boldsymbol{U}}_n^{(\ell)}\,] \tilde{\boldsymbol{\Sigma}}^{(\ell)} \tilde{\boldsymbol{V}}^{(\ell)^{\mathrm{H}}}, \tag{11}$$

where $\tilde{\boldsymbol{U}}_n^{(\ell)}$ contains the last $(M_{\mathrm{R}} - \tilde{L}^{(\ell)})$ left singular vectors. Thus, $\tilde{\boldsymbol{U}}_n^{(\ell)}$ forms an orthogonal basis for the left null space of $\tilde{\boldsymbol{H}}^{(\ell)}$ such that $\tilde{\boldsymbol{U}}_n^{(\ell)^{\mathrm{H}}} \tilde{\boldsymbol{H}}^{(\ell)} = \boldsymbol{0}$. Then a linear combination of the rows of $\tilde{\boldsymbol{U}}_n^{(\ell)^{\mathrm{H}}}$ are the candidate for the receive filter $\boldsymbol{G}_{\mathrm{R}}^{(\ell)}$. Unlike the work in [21], we choose

$$\boldsymbol{G}_{\mathrm{R}}^{(\ell)} = \tilde{\boldsymbol{U}}_n^{(\ell)} \tilde{\boldsymbol{U}}_n^{(\ell)^{\mathrm{H}}} \in \mathbb{C}^{M_{\mathrm{R}} \times M_{\mathrm{R}}}. \tag{12}$$

It can be easily seen that the $\boldsymbol{G}_{\mathrm{R}}^{(\ell)}$ in (12) is a projection matrix which projects any matrix onto the left null space of $\tilde{\boldsymbol{H}}^{(\ell)}$.

[3]The scaling issue is due to the power control solution at the relay which is explained in Section III.

In the BC phase, due to the reciprocity of the channel and the usage of BD, the transmit filter $\boldsymbol{G}_{\mathrm{T}}^{(\ell)}$ and receive filter $\boldsymbol{G}_{\mathrm{R}}^{(\ell)}$ are also reciprocal, so that we get

$$\boldsymbol{G}_{\mathrm{T}}^{(\ell)} = \boldsymbol{G}_{\mathrm{R}}^{(\ell)^{\mathrm{T}}}. \tag{13}$$

Note that the BD inspired strategy can null the inter-operator interference completely. However, it is restricted by the dimensionality constraint, i.e., the left null space of $\tilde{\boldsymbol{H}}^{(\ell)}$ cannot be empty. For our system it implies that the condition $M_{\mathrm{R}} > 2(L-1)M_{\mathrm{U}}$ has to be fulfilled.

B. Regularized Block-Diagonalization at the Relay

One algorithm for MU-MIMO systems which is not limited by the dimensionality constraint is the RBD algorithm [20]. It allows a residual amount of interference in order to balance it with the noise enhancement. It has been also proved in [18] that the performance of RBD converges to BD in the high SNR regime. Now we adopt the RBD design for our scenario.

In the MAC phase, the mean square error (MSE) of the received signal vector can be written as:

$$\begin{aligned}
&\mathbb{E}\left\{\|\boldsymbol{x} - \boldsymbol{G}_{\mathrm{R}}\boldsymbol{r}\|^2\right\} \\
&\quad = \mathbb{E}\left\{\|\boldsymbol{x} - \boldsymbol{G}_{\mathrm{R}}\boldsymbol{H}\boldsymbol{x} - \boldsymbol{G}_{\mathrm{R}}\boldsymbol{n}_{\mathrm{R}}\|^2\right\} \\
&\quad = \mathbb{E}\left\{\|\boldsymbol{x} - \boldsymbol{G}_{\mathrm{R}}\boldsymbol{H}\boldsymbol{x}\|^2 + \|\boldsymbol{G}_{\mathrm{R}}\boldsymbol{n}_{\mathrm{R}}\|^2\right\}
\end{aligned} \tag{14}$$

where $\boldsymbol{x} = [\boldsymbol{x}_1^{(1)^{\mathrm{T}}}, \boldsymbol{x}_2^{(1)^{\mathrm{T}}}, \ldots \boldsymbol{x}_1^{(L)^{\mathrm{T}}}, \boldsymbol{x}_2^{(L)^{\mathrm{T}}}]^{\mathrm{T}} \in \mathbb{C}^{2LM_{\mathrm{U}}}$ contains the concatenated transmitted signal vectors of all the UTs and the equivalent combined channel matrix of all the operators $\boldsymbol{G}_{\mathrm{R}}\boldsymbol{H}$ is equal to

$$\boldsymbol{G}_{\mathrm{R}}\boldsymbol{H} = \begin{bmatrix}
\boldsymbol{G}_{\mathrm{R}}^{(1)}\boldsymbol{H}^{(1)} & \boldsymbol{G}_{\mathrm{R}}^{(1)}\boldsymbol{H}^{(2)} & \ldots & \boldsymbol{G}_{\mathrm{R}}^{(1)}\boldsymbol{H}^{(L)} \\
\boldsymbol{G}_{\mathrm{R}}^{(2)}\boldsymbol{H}^{(1)} & \boldsymbol{G}_{\mathrm{R}}^{(2)}\boldsymbol{H}^{(2)} & \ldots & \boldsymbol{G}_{\mathrm{R}}^{(2)}\boldsymbol{H}^{(L)} \\
\vdots & \vdots & \ddots & \vdots \\
\boldsymbol{G}_{\mathrm{R}}^{(L)}\boldsymbol{H}^{(1)} & \boldsymbol{G}_{\mathrm{R}}^{(L)}\boldsymbol{H}^{(2)} & \ldots & \boldsymbol{G}_{\mathrm{R}}^{(L)}\boldsymbol{H}^{(L)}
\end{bmatrix}. \tag{15}$$

Using the same definition of the interference channel $\tilde{\boldsymbol{H}}^{(\ell)}$ as in (10), the ℓth operator's effective channel is given by $\boldsymbol{G}_{\mathrm{R}}^{(\ell)}\boldsymbol{H}^{(\ell)}$ and the interference caused by the other operators to the ℓth operator is determined by $\boldsymbol{G}_{\mathrm{R}}^{(\ell)}\tilde{\boldsymbol{H}}^{(\ell)}$. Inspired by the RBD algorithm, the matrix $\boldsymbol{G}_{\mathrm{R}}$ is designed to minimize the interference plus noise power, i.e., the optimization criterion of our RBD inspired strategy is given as

$$\boldsymbol{G}_{\mathrm{R}} = \arg\min_{\boldsymbol{G}_{\mathrm{R}}} \mathbb{E}\left\{\sum_{\ell=1}^{L}\left\|\boldsymbol{G}_{\mathrm{R}}^{(\ell)}\tilde{\boldsymbol{H}}^{(\ell)}\tilde{\boldsymbol{x}}^{(\ell)}\right\|^2 + \|\boldsymbol{G}_{\mathrm{R}}\boldsymbol{n}_{\mathrm{R}}\|^2\right\} \tag{16}$$

where $\tilde{\boldsymbol{x}}^{(\ell)} = \left[\boldsymbol{x}^{(1)^{\mathrm{T}}} \ldots \boldsymbol{x}^{(\ell-1)^{\mathrm{T}}} \boldsymbol{x}^{(\ell+1)^{\mathrm{T}}} \ldots \boldsymbol{x}^{(L)^{\mathrm{T}}}\right]^{\mathrm{T}}$ with $\boldsymbol{x}^{(\ell)} = \left[\boldsymbol{x}_1^{(\ell)^{\mathrm{T}}} \; \boldsymbol{x}_2^{(\ell)^{\mathrm{T}}}\right]^{\mathrm{T}}$.

Let us again compute the SVD of $\tilde{\boldsymbol{H}}^{(\ell)}$ as

$$\tilde{\boldsymbol{H}}^{(\ell)} = \tilde{\boldsymbol{U}}^{(\ell)}\tilde{\boldsymbol{\Sigma}}^{(\ell)}\tilde{\boldsymbol{V}}^{(\ell)^{\mathrm{H}}}. \tag{17}$$

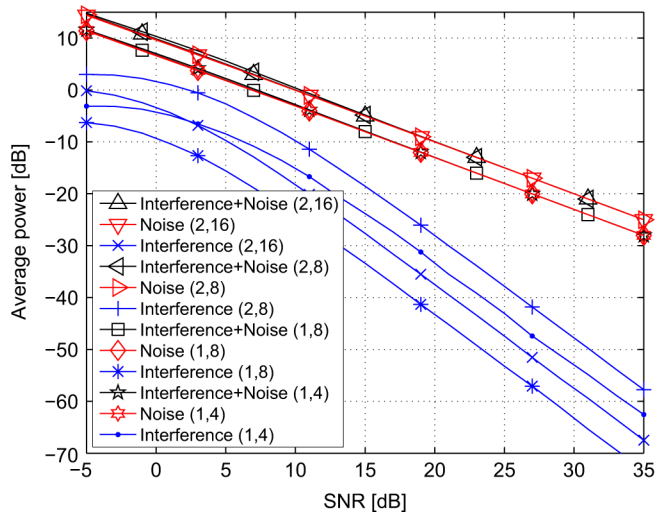

Fig. 3. The average interference level when RBD is applied and $L = 2$. (2,16) stands for $(M_{\mathrm{U}},\ M_{\mathrm{R}})$. SNR is defined as in Section VI.

Following a similar procedure as in [20], the solution to (16) can be obtained as

$$\boldsymbol{G}_{\mathrm{R}}^{(\ell)} = \left(\frac{P_k^{(\ell)}}{M_{\mathrm{U}}}\tilde{\boldsymbol{\Sigma}}^{(\ell)}\tilde{\boldsymbol{\Sigma}}^{(\ell)^{\mathrm{H}}} + \sigma_{\mathrm{R}}^2\boldsymbol{I}_{M_{\mathrm{R}}}\right)^{-\frac{1}{2}}\tilde{\boldsymbol{U}}^{(\ell)^{\mathrm{H}}}. \tag{18}$$

The complete proof is given in the Appendix A.

In the BC phase, the design of the $\boldsymbol{G}_{\mathrm{T}}$ matrix follows the same way. The interference generated to the other operators is determined by $\tilde{\boldsymbol{H}}^{(\ell)^{\mathrm{T}}}\boldsymbol{G}_{\mathrm{T}}^{(\ell)}$.[4] Then, the optimization criterion becomes

$$\boldsymbol{G}_{\mathrm{T}} = \arg\min_{\boldsymbol{G}_{\mathrm{T}}} \mathbb{E}\left\{\sum_{\ell=1}^{L}\left(\left\|\tilde{\boldsymbol{H}}^{(\ell)^{\mathrm{T}}}\boldsymbol{G}_{\mathrm{T}}^{(\ell)}\tilde{\boldsymbol{x}}^{(\ell)}\right\|^2 + \left\|\boldsymbol{n}^{(\ell)}\right\|^2\right)\right\}, \tag{19}$$

where $\boldsymbol{n}^{(\ell)} = \left[\boldsymbol{n}_1^{(\ell)^{\mathrm{T}}} \; \boldsymbol{n}_2^{(\ell)^{\mathrm{T}}}\right]^{\mathrm{T}}$ and we set $\sum_{\ell=1}^{L}\|\boldsymbol{G}_{\mathrm{T}}^{(\ell)}\|_{\mathrm{F}}^2 = P_{\mathrm{R}}$. After following the optimization procedure in [20] and utilizing the SVD definition in (17), $\boldsymbol{G}_{\mathrm{T}}^{(\ell)}$ is obtained as

$$\boldsymbol{G}_{\mathrm{T}}^{(\ell)} = \tilde{\boldsymbol{U}}^{(\ell)^*}\left(\tilde{\boldsymbol{\Sigma}}^{(\ell)^*}\tilde{\boldsymbol{\Sigma}}^{(\ell)^{\mathrm{T}}} + 2LM_{\mathrm{U}}\sigma_k^{(\ell)^2}\frac{\boldsymbol{I}_{M_{\mathrm{R}}}}{P_{\mathrm{R}}}\right)^{-\frac{1}{2}}. \tag{20}$$

Fig. 3 demonstrates the relationship between the residual interference power and the effective noise power when the RBD inspired strategy is applied. It is obvious that the residual interference decreases significantly as SNR increases. This implies that the RBD inspired design is noise dominated especially in the high SNR regime for our application.

C. Relay Amplification Matrix for Each Subsystem

After applying the receive filter $\boldsymbol{G}_{\mathrm{R}}$ and the transmit filter $\boldsymbol{G}_{\mathrm{T}}$, we get L independent single-operator TWR systems when BD is used which corresponds to RBD in the high SNR regime. Thus, each submatrix $\boldsymbol{G}_{\mathrm{S}}^{(\ell)}$ can be derived separately. In general, any arbitrary design of $\boldsymbol{G}_{\mathrm{S}}^{(\ell)}$ can be applied. Nevertheless, in our work we use the ANOMAX transmit strategy where the

[4] $\{\cdot\}^{\mathrm{T}}$ comes from the reciprocity assumption.

Frobenius norm of the desired signal is maximized [14] and its modification RR-ANOMAX which restores the rank while preserving the same subspace and is thus more suitable for spatial multiplexing [15]. Both algorithms have a good trade-off between performance and computational complexity.

The received signal vectors (4) at the UTs of the ℓth operator can be further expanded as

$$\begin{aligned}\boldsymbol{y}_1^{(\ell)} &= \boldsymbol{H}_{1,1}^{(\ell)}\boldsymbol{x}_1^{(\ell)} + \boldsymbol{H}_{1,2}^{(\ell)}\boldsymbol{x}_2^{(\ell)} + \tilde{\boldsymbol{n}}_1^{(\ell)} \\ \boldsymbol{y}_2^{(\ell)} &= \boldsymbol{H}_{2,2}^{(\ell)}\boldsymbol{x}_2^{(\ell)} + \boldsymbol{H}_{2,1}^{(\ell)}\boldsymbol{x}_1^{(\ell)} + \tilde{\boldsymbol{n}}_2^{(\ell)},\end{aligned} \tag{21}$$

where $\tilde{\boldsymbol{n}}_k^{(\ell)} = \sum_{\bar{k},\bar{\ell}\neq\ell} \boldsymbol{H}_k^{(\ell)^{\mathrm{T}}}\boldsymbol{G}\boldsymbol{H}_{\bar{k}}^{(\bar{\ell})}\boldsymbol{x}_{\bar{k}}^{(\bar{\ell})} + \boldsymbol{H}_k^{(\ell)^{\mathrm{T}}}\boldsymbol{G}\boldsymbol{n}_{\mathrm{R}} + \boldsymbol{n}_k^{(\ell)}$ denotes the effective noise term which consists of the residual inter-operator interference, the UTs' own noise, and the forwarded relay noise. The effective channel $\boldsymbol{H}_{k,m}^{(\ell)}$ between the source m and destination k is defined as

$$\boldsymbol{H}_{k,m}^{(\ell)} = \boldsymbol{H}_k^{(\ell)^{\mathrm{T}}}\boldsymbol{G}_{\mathrm{T}}^{(\ell)}\boldsymbol{G}_{\mathrm{S}}^{(\ell)}\boldsymbol{G}_{\mathrm{R}}^{(\ell)}\boldsymbol{H}_m^{(\ell)}, \tag{22}$$

where $m \in \{1,2\}$. The ANOMAX algorithm solves the following cost function [14]

$$\arg \max_{\left\|\boldsymbol{G}_{\mathrm{S}}^{(\ell)}\right\|_{\mathrm{F}}=1} \beta^2 \left\|\boldsymbol{H}_{1,2}^{(\ell)}\right\|_{\mathrm{F}}^2 + (1-\beta)^2 \left\|\boldsymbol{H}_{2,1}^{(\ell)}\right\|_{\mathrm{F}}^2 \tag{23}$$

where $\beta \in [0,1]$ is a weighting factor. Next we introduce the definitions $\boldsymbol{g}_{\mathrm{S}}^{(\ell)} = \mathrm{vec}\{\boldsymbol{G}_{\mathrm{S}}^{(\ell)}\}$ and

$$\boldsymbol{K}_{\beta}^{(\ell)} = \Big[\beta((\boldsymbol{G}_{\mathrm{R}}^{(\ell)}\boldsymbol{H}_2^{(\ell)}) \otimes (\boldsymbol{G}_{\mathrm{T}}^{(\ell)^{\mathrm{T}}}\boldsymbol{H}_1^{(\ell)})), \quad (1-\beta)\left((\boldsymbol{G}_{\mathrm{R}}^{(\ell)}\boldsymbol{H}_1^{(\ell)}) \otimes (\boldsymbol{G}_{\mathrm{T}}^{(\ell)^{\mathrm{T}}}\boldsymbol{H}_2^{(\ell)})\right)\Big]. \tag{24}$$

We compute the SVD of $\boldsymbol{K}_{\beta}^{(\ell)}$ as $\boldsymbol{K}_{\beta}^{(\ell)} = \boldsymbol{U}_{\beta}^{(\ell)}\boldsymbol{\Sigma}_{\beta}^{(\ell)}\boldsymbol{V}_{\beta}^{(\ell)^{\mathrm{H}}}$. Then, the optimal $\boldsymbol{g}_{\mathrm{S}}^{(\ell)}$ is given by $\boldsymbol{g}_{\mathrm{S}}^{(\ell)} = \boldsymbol{u}_{\beta,1}^{(\ell)^*}$, where $\boldsymbol{u}_{\beta,1}^{(\ell)}$ is the first column of $\boldsymbol{U}_{\beta}^{(\ell)}$[14]. Finally, the optimal matrix $\boldsymbol{G}_{\mathrm{S}}^{(\ell)}$ is computed via

$$\boldsymbol{G}_{\mathrm{S}}^{(\ell)} = \mathrm{unvec}_{M_{\mathrm{R}}\times M_{\mathrm{R}}}\left\{\boldsymbol{u}_{\beta,1}^{(\ell)^*}\right\}. \tag{25}$$

However, as discussed in [15], the ANOMAX scheme yields a low rank relay amplification matrix and therefore cannot reach the full multiplexing gain for high SNRs especially when multiple antennas are deployed at the UTs. Therefore, one alternate low complexity scheme which is called water-filling rank-restored ANOMAX (WF RR-ANOMAX) is proposed in the same paper. The WF RR-ANOMAX scheme restores the rank of the relay amplification matrix $\boldsymbol{G}_{\mathrm{S}}^{(\ell)}$ via an optimization inspired by the water filling algorithm over the profile of the singular values of the matrix $\boldsymbol{G}_{\mathrm{S}}^{(\ell)}$[15].

D. Transmit and Receive Strategies at the UTs

When each UT has multiple antennas, it is beneficial to apply the precoding matrix to either exploit the multiplexing gain or the diversity gain. Beamforming designs have also been addressed in [7]. The beamforming schemes used in [7] are based on the amount of channel state information (CSI) available at the UTs. Moreover, in [7] $\boldsymbol{H}_k^{(\ell)}$ is required for each UT to generate its beamforming vector. However, it is more natural to design the beamforming vector based on the equivalent channel between the transceiver pair, i.e., the pair of UTs which communicate with each other. It is also easier to obtain the equivalent channel than to obtain $\boldsymbol{H}_k^{(\ell)}$ at each UT as shown in Section V.

TABLE I
ITERATIVE POWER CONTROL AT THE RELAY IN CASE OF MULTI-STREAM TRANSMISSION

Initialization step: set $\gamma_0^{(0)} = 1$, $\boldsymbol{G}_0^{(0)} = \boldsymbol{G}_0$, maximum iteration number $N_{\max}$ and the threshold value ϵ.

Main step:

for $p = 1$ to $N_{\max}$ **do**
  Insert $\boldsymbol{G}_0^{(p-1)}$ into the algorithm in Appendix B to calculate $\boldsymbol{R}_{\boldsymbol{x}_k^{(\ell)}\boldsymbol{x}_k^{(\ell)}}^{(p)}$.
  Insert $\boldsymbol{R}_{\boldsymbol{x}_k^{(\ell)}\boldsymbol{x}_k^{(\ell)}}^{(p)}$ and $\boldsymbol{G}_0^{(p-1)}$ into equation (26) to obtain $\gamma_{\mathrm{update}}^{(p)}$.
  $\gamma_0^{(p)} = \gamma_0^{(p-1)} \cdot \gamma_{\mathrm{update}}^{(p)}$
  $\boldsymbol{G}_0^{(p)} = \gamma_0^{(p)}\boldsymbol{G}_0$
  if $|\log_{10}(\gamma_{\mathrm{update}}^{(p)})| < \epsilon$ **then**
    $\boldsymbol{G} = \gamma_0^{(p)} \cdot \boldsymbol{G}_0$
    break
  end if
end for

Since the transmit and receive strategies of the same UT are based on different equivalent channels, we define two kinds of equivalent channels. The first one, which we refer to as the equivalent forward channel, denotes the effective channel from the source to the destination. The second one, which we refer to as the equivalent backward channel, denotes the effective channel measured at the destination from the source. Taking UTs of the ℓth operator as an example, the equivalent forward channel of its first UT is $\boldsymbol{H}_2^{(\ell)^{\mathrm{T}}}\boldsymbol{G}\boldsymbol{H}_1^{(\ell)}$ and its corresponding equivalent backward channel is $\boldsymbol{H}_1^{(\ell)^{\mathrm{T}}}\boldsymbol{G}\boldsymbol{H}_2^{(\ell)}$. Assume that ProBaSeMO is used to determine $\boldsymbol{G}$ and we fix $\boldsymbol{G}_0$ during the training phase and the data transmission phase. The resulting system will comprise $2L$ independent point-to-point MIMO systems.[5] In our work, the matrices $\boldsymbol{W}_k^{(\ell)}$ and $\boldsymbol{F}_k^{(\ell)}$ are designed using two optimal transmit strategies for single stream transmission and multiple stream transmission in the point-to-point MIMO system, respectively.

- **Dominant eigenmode transmission (DET)**: The transmit and receive beamforming vectors of the effective channel between the transceiver pair are chosen to be its right and left dominant singular vector, respectively. DET is a single stream transmission scheme which maximizes the receive SNR.
- **Spatial multiplexing with water-filling algorithm (WF)**: With perfect CSI at the transmitter the capacity maximizing spatial multiplexing strategy corresponds to the SVD based precoding along with a power allocation based on water-filling [12].

Note that all the point-to-point MIMO systems experience colored noise. Therefore, prewhitening operation is required. The details on the DET and WF schemes are shown in Appendix B.

[5]For RBD the residual inter-operator interference is treated as noise.

TABLE II
COMPARISON OF RELAY AMPLIFICATION SCHEMES

Algorithm	$\boldsymbol{G}_{\mathrm{T}}$	$\boldsymbol{G}_{\mathrm{S}}$	$\boldsymbol{G}_{\mathrm{R}}$
ZF [7]	$(\boldsymbol{F}\boldsymbol{H}^{\mathrm{T}})^{\mathrm{H}}\left((\boldsymbol{F}\boldsymbol{H}^{\mathrm{T}})(\boldsymbol{F}\boldsymbol{H}^{\mathrm{T}})^{\mathrm{H}}\right)^{-1}$	$\boldsymbol{I}_L \otimes (\boldsymbol{\Pi}_2 \otimes \boldsymbol{I}_{M_{\mathrm{U}}})$	$\left((\boldsymbol{H}\boldsymbol{W})^{\mathrm{H}}(\boldsymbol{H}\boldsymbol{W})\right)^{-1}(\boldsymbol{H}\boldsymbol{W})^{\mathrm{H}}$
MMSE [7]	$\left(\boldsymbol{H}^{\mathrm{H}^{\mathrm{T}}}\boldsymbol{F}^{\mathrm{H}}\boldsymbol{F}\boldsymbol{H}^{\mathrm{T}} + 2L{\sigma_k^{(\ell)}}^2\boldsymbol{I}_{M_{\mathrm{R}}}/P_{\mathrm{R}}\right)^{-1}\boldsymbol{H}^{\mathrm{T}}\boldsymbol{F}^{\mathrm{H}}$	$\boldsymbol{I}_L \otimes (\boldsymbol{\Pi}_2 \otimes \boldsymbol{I}_{M_{\mathrm{U}}})$	$\boldsymbol{W}^{\mathrm{H}}\boldsymbol{H}^{\mathrm{H}}\left(\boldsymbol{H}\boldsymbol{W}\boldsymbol{W}^{\mathrm{H}}\boldsymbol{H}^{\mathrm{T}} + \sigma_{\mathrm{R}}^2\boldsymbol{I}_{M_{\mathrm{R}}}/P_k^{(\ell)}\right)^{-1}$
ProBaSeMO (BD)	$\boldsymbol{G}_{\mathrm{R}}^{\mathrm{T}}$	Arbitrary block diagonal matrix	$\tilde{\boldsymbol{U}}_{\mathrm{n}}^{(\ell)}\tilde{\boldsymbol{U}}_{\mathrm{n}}^{(\ell)^{\mathrm{H}}}\forall\ell$
ProBaSeMO (RBD)	$\tilde{\boldsymbol{U}}^{(\ell)^*}\left(\tilde{\boldsymbol{\Sigma}}^{(\ell)^*}\tilde{\boldsymbol{\Sigma}}^{(\ell)^{\mathrm{T}}} + 2LM_{\mathrm{U}}{\sigma_k^{(\ell)}}^2\boldsymbol{I}_{M_{\mathrm{R}}}/P_{\mathrm{R}}\right)^{-1/2},\forall\ell$	Arbitrary block diagonal matrix	$\left(P_k^{(\ell)}\tilde{\boldsymbol{\Sigma}}^{(\ell)}\tilde{\boldsymbol{\Sigma}}^{(\ell)^{\mathrm{H}}}/M_{\mathrm{U}} + \sigma_{\mathrm{R}}^2\boldsymbol{I}_{M_{\mathrm{R}}}\right)^{-1/2}\tilde{\boldsymbol{U}}^{(\ell)^{\mathrm{H}}},\forall\ell$

E. Power Control at the Relay

In this section, we determine the amplification factor γ_0 which scales $\boldsymbol{G}_0$ such that the transmit power constraint at the relay is fulfilled. The amplification factor γ_0 can be obtained via

$$\gamma_0 = \sqrt{\frac{P_{\mathrm{R}}}{\mathbb{E}\{\|\bar{\boldsymbol{r}}\|^2\}}} = \sqrt{\frac{P_{\mathrm{R}}}{\mathrm{Tr}\left\{\boldsymbol{G}_0\left(\sum_{k,\ell}P_k^{(\ell)}\boldsymbol{Q}_k^{(\ell)} + \sigma_{\mathrm{R}}^2\boldsymbol{I}_{M_{\mathrm{R}}}\right)\boldsymbol{G}_0^{\mathrm{H}}\right\}}} \quad (26)$$

with $\boldsymbol{Q}_k^{(\ell)} = \boldsymbol{H}_k^{(\ell)}\boldsymbol{R}_{\boldsymbol{x}_k^{(\ell)}\boldsymbol{x}_k^{(\ell)}}\boldsymbol{H}_k^{(\boldsymbol{\ell})^{\mathrm{H}}}$. Here the transmit covariance matrix of the kth UT of the ℓth operator is defined as $\boldsymbol{R}_{\boldsymbol{x}_k^{(\boldsymbol{\ell})}\boldsymbol{x}_k^{(\boldsymbol{\ell})}} = \boldsymbol{W}_k^{(\ell)}\boldsymbol{W}_k^{(\ell)^{\mathrm{H}}}$.

However, when the transmit strategies in Section III-D are used, γ_0 cannot be calculated in a closed-form using (26). This is due to the fact that in general the precoding matrices (e.g., WF) of the UTs depend on the the effective SNR which is a function of γ_0. Vice versa, the power allocation at each UT will affect $\mathrm{Tr}\{\boldsymbol{G}_0P_k^{(\ell)}\boldsymbol{Q}_k^{(\ell)}\boldsymbol{G}_0^{\mathrm{H}}\}$ and thus the received power at the relay. Hence, to fulfill the transmit power constraint at the relay a joint design of $\boldsymbol{R}_{\boldsymbol{x}_k^{(\boldsymbol{\ell})}\boldsymbol{x}_k^{(\boldsymbol{\ell})}}$ and γ_0 is required. To avoid a complex joint optimization, we propose an iterative solution which finds the two parameters sequentially. The proposed iterative algorithm is presented in Table I.

Remarks

Remark 1: As shown in [14], if the weighting factor β is set to 0.5, we will have $\boldsymbol{G}_{\mathrm{S}}^{(\ell)} = \boldsymbol{G}_{\mathrm{S}}^{(\ell)^{\mathrm{T}}}$. Furthermore, if BD is applied or RBD is applied in the high SNR regime, we get $\boldsymbol{G} = \boldsymbol{G}^{\mathrm{T}}$. Such a feature can help to avoid the use of channel feedback or backhauling when channel reciprocity exists. Thus it further reduces the complexity of the system.

Remark 2: The ZF and MMSE solution in [7] can be also obtained using the routine of (7), i.e., designing $\boldsymbol{G}_{\mathrm{T}}$ and $\boldsymbol{G}_{\mathrm{R}}$ using the ZF and MMSE criteria. Since in these cases all the channels are equalized, the matrix $\boldsymbol{G}_{\mathrm{S}}^{(\ell)} = \boldsymbol{\Pi}_2 \otimes \boldsymbol{I}_{M_{\mathrm{U}}}$ is a permutation matrix where $\boldsymbol{\Pi}_2 = \begin{bmatrix}0 & 1\\ 1 & 0\end{bmatrix}$ is the exchange matrix which ensures that the user will not receive its own transmitted data. A detailed comparison is shown in Table II. Note that the ZF algorithm requires that $M_{\mathrm{R}} \geq 2LM_{\mathrm{U}}$ if the same transmit strategy is used.

Remark 3: The problem of jointly designing $\boldsymbol{G}$, $\boldsymbol{W}_k^{(\ell)}$, and $\boldsymbol{F}_k^{(\ell)}$ is non-convex. To simplify the non-convexity, iteratively designing these matrices using the strategy in Section III can improve the performance. However, this requires an additional overhead in both signaling and computational complexity compared to the proposed scheme.

IV. SUM RATE MAXIMIZAION

In this section, we derive the matrix $\boldsymbol{G}$ using the sum rate maximization criterion. Then, the results will be used as the benchmark for our ProBaSeMO scheme.

A. Single Antenna at Each UT

We compute the optimal $\boldsymbol{G}$ which maximizes the sum rate of the system subject to a transmit power constraint at the relay, i.e.,

$$\begin{aligned}\max_{\boldsymbol{G}} \quad & \frac{1}{2}\sum_{\ell=1}^{L}\sum_{k=1}^{2}\log_2(1+\eta_k^{(\ell)})\\ \text{subject to} \quad & \mathbb{E}\{\|\bar{\boldsymbol{r}}\|^2\} \leq P_{\mathrm{R}}.\end{aligned} \quad (27)$$

Since each UT has only a single antenna, the SINR $\eta_k^{(\ell)}$ of each UT is expressed as

$$\eta_k^{(\ell)} = \frac{\mathbb{E}\{|\boldsymbol{h}_k^{(\ell)^{\mathrm{T}}}\boldsymbol{G}\boldsymbol{h}_{3-k}^{(\ell)}x_{3-k}^{(\ell)}|^2\}}{\mathbb{E}\left\{\left|\sum_{\bar{k},\bar{\ell}\neq\ell}\boldsymbol{h}_k^{(\ell)^{\mathrm{T}}}\boldsymbol{G}\boldsymbol{h}_{\bar{k}}^{(\bar{\ell})}x_{\bar{k}}^{(\bar{\ell})}\right|^2\right\} + \mathbb{E}\{\|\boldsymbol{h}_k^{(\ell)^{\mathrm{T}}}\boldsymbol{G}\boldsymbol{n}_{\mathrm{R}}\|^2\} + \sigma_k^{(\ell)^2}} \quad (28)$$

where all the terms in (28) come from the single antenna version of (4).

To derive the optimal $\boldsymbol{G}$, further algebraic manipulations are required. The transmit power at the relay can be expanded as

$$\begin{aligned}&\mathbb{E}\{\|\bar{\boldsymbol{r}}\|^2\}\\ &= \mathbb{E}\{\mathrm{Tr}\{\boldsymbol{G}\boldsymbol{r}(\boldsymbol{G}\boldsymbol{r})^{\mathrm{H}}\}\}\\ &= \mathrm{Tr}\left\{\boldsymbol{G}\left(\sum_{k,\ell}P_k^{(\ell)}\boldsymbol{h}_k^{(\ell)}\boldsymbol{h}_k^{(\ell)^{\mathrm{H}}} + \sigma_{\mathrm{R}}^2\boldsymbol{I}_{M_{\mathrm{R}}}\right)\boldsymbol{G}^{\mathrm{H}}\right\}\\ &= \sum_{k,\ell}\mathrm{Tr}\left\{P_k^{(\ell)}\boldsymbol{G}\boldsymbol{h}_k^{(\ell)}\boldsymbol{h}_k^{(\ell)^{\mathrm{H}}}\boldsymbol{G}^{\mathrm{H}}\right\} + \mathrm{Tr}\left\{\sigma_{\mathrm{R}}^2\boldsymbol{G}\boldsymbol{G}^{\mathrm{H}}\right\}\\ &= \sum_{k,\ell}P_k^{(\ell)}(\boldsymbol{G}\boldsymbol{h}_k^{(\ell)})^{\mathrm{H}}\boldsymbol{G}\boldsymbol{h}_k^{(\ell)} + \sigma_{\mathrm{R}}^2\boldsymbol{g}^{\mathrm{H}}\boldsymbol{g}\\ &= \boldsymbol{g}^{\mathrm{H}}\boldsymbol{\Lambda}\boldsymbol{g}\end{aligned} \quad (29)$$

where $\boldsymbol{g} = \mathrm{vec}\{\boldsymbol{G}\}$. The fact $\mathrm{Tr}\{\boldsymbol{\Gamma}\boldsymbol{\zeta}\} = \mathrm{Tr}\{\boldsymbol{\zeta}\boldsymbol{\Gamma}\}$ and $\mathrm{vec}\{\boldsymbol{\Gamma}\boldsymbol{X}\boldsymbol{\zeta}\} = (\boldsymbol{\zeta}^{\mathrm{T}} \otimes \boldsymbol{\Gamma})\mathrm{vec}\{\boldsymbol{X}\}$ is used in the derivation. Moreover, $\boldsymbol{\Lambda}$ is a positive definite Hermitian matrix which is defined as

$$\boldsymbol{\Lambda} = \sum_{k,\ell}P_k^{(\ell)}((\boldsymbol{h}_k^{(\ell)}\boldsymbol{h}_k^{(\ell)^{\mathrm{H}}})^{\mathrm{T}} \otimes \boldsymbol{I}_{M_{\mathrm{R}}}) + \sigma_{\mathrm{R}}^2\boldsymbol{I}_{M_{\mathrm{R}}^2}. \quad (30)$$

Following a similar procedure, the SINR $\eta_k^{(\ell)}$ can be rewritten as

$$\eta_k^{(\ell)} = \frac{\boldsymbol{g}^{\mathrm{H}}\boldsymbol{\Phi}_k^{(\ell)}\boldsymbol{g}}{\boldsymbol{g}^{\mathrm{H}}(\boldsymbol{\Upsilon}_k^{(\ell)} + \boldsymbol{\Delta}_k^{(\ell)})\boldsymbol{g} + {\sigma_k^{(\ell)}}^2} \tag{31}$$

where $\boldsymbol{\Phi}_k^{(\ell)}$, $\boldsymbol{\Upsilon}_k^{(\ell)}$, and $\boldsymbol{\Delta}_k^{(\ell)}$ are defined as

$$\begin{aligned}
\boldsymbol{\Phi}_k^{(\ell)} &= P_k^{(\ell)}(\boldsymbol{h}_{3-k}^{(\ell)^{\mathrm{T}}} \otimes \boldsymbol{h}_k^{(\ell)^{\mathrm{T}}})^{\mathrm{H}}(\boldsymbol{h}_{3-k}^{(\ell)^{\mathrm{T}}} \otimes \boldsymbol{h}_k^{(\ell)^{\mathrm{T}}}) \\
\boldsymbol{\Upsilon}_k^{(\ell)} &= \sum_{\bar{k},\bar{\ell}\neq\ell} P_{\bar{k}}^{(\bar{\ell})}(\boldsymbol{h}_{\bar{k}}^{(\bar{\ell})^{\mathrm{T}}} \otimes \boldsymbol{h}_k^{(\ell)^{\mathrm{T}}})^{\mathrm{H}}(\boldsymbol{h}_{\bar{k}}^{(\bar{\ell})^{\mathrm{T}}} \otimes \boldsymbol{h}_k^{(\ell)^{\mathrm{T}}}) \\
\boldsymbol{\Delta}_k^{(\ell)} &= \sigma_{\mathrm{R}}^2(\boldsymbol{I}_{M_{\mathrm{R}}} \otimes (\boldsymbol{h}_k^{(\ell)}\boldsymbol{h}_k^{(\ell)^{\mathrm{H}}})^{\mathrm{T}}).
\end{aligned} \tag{32}$$

The derivation of (31) is found in Appendix C.

Inserting (31) and (29) into (27), the original problem can be reformulated as

$$\begin{aligned}
\max_{\boldsymbol{g}} \quad & \frac{1}{2}\sum_{k,\ell}\log_2\left(1 + \frac{\boldsymbol{g}^{\mathrm{H}}\boldsymbol{\Phi}_k^{(\ell)}\boldsymbol{g}}{\boldsymbol{g}^{\mathrm{H}}(\boldsymbol{\Upsilon}_k^{(\ell)} + \boldsymbol{\Delta}_k^{(\ell)})\boldsymbol{g} + {\sigma_k^{(\ell)}}^2}\right) \\
\text{subject to} \quad & \boldsymbol{g}^{\mathrm{H}}\boldsymbol{\Lambda}\boldsymbol{g} \leq P_{\mathrm{R}}.
\end{aligned} \tag{33}$$

Problem (33) is non-convex. To simplify the optimization problem we note that the inequality constraint in (33) has to be satisfied with equality at the optimal point. Otherwise, the optimal $\boldsymbol{g}$ can be scaled up to satisfy the constraint with equality while increasing the objective function, which contradicts the optimality. Inserting the power constraint into the objective function, problem (33) can be reformulated as an unconstrained optimization problem

$$\max_{\boldsymbol{g}} \quad \lambda(\boldsymbol{g}) = \prod_{\ell=1}^{L}\prod_{k=1}^{2}\frac{\boldsymbol{g}^{\mathrm{H}}\boldsymbol{A}_k^{(\ell)}\boldsymbol{g}}{\boldsymbol{g}^{\mathrm{H}}\boldsymbol{C}_k^{(\ell)}\boldsymbol{g}} \tag{34}$$

where $\boldsymbol{C}_k^{(\ell)} = \boldsymbol{\Upsilon}_k^{(\ell)} + \boldsymbol{\Delta}_k^{(\ell)} + \frac{{\sigma_k^{(\ell)}}^2}{P_{\mathrm{R}}}\boldsymbol{\Lambda}$ and $\boldsymbol{A}_k^{(\ell)} = \boldsymbol{C}_k^{(\ell)} + \boldsymbol{\Phi}_k^{(\ell)}$ are positive definite Hermitian matrices. Since the objective function in (34) is homogeneous and any scaling in $\boldsymbol{g}$ does not change the optimality, the solution to problem (34) differs from the solution to (27) only in scaling and reshaping, i.e., if $\bar{\boldsymbol{g}}$ is the solution to (34), the optimal solution to (27) is given by

$$\boldsymbol{G} = \mathrm{unvec}_{M_{\mathrm{R}}\times M_{\mathrm{R}}}\left\{\bar{\boldsymbol{g}}\sqrt{\frac{P_{\mathrm{R}}}{\bar{\boldsymbol{g}}^{\mathrm{H}}\boldsymbol{\Lambda}\bar{\boldsymbol{g}}}}\right\}. \tag{35}$$

To solve (34), we follow a similar routine as in [16]. We take the necessary condition for optimality of (34), i.e.,

$$\frac{\partial\lambda(\boldsymbol{g})}{\partial\boldsymbol{g}^*} = 0. \tag{36}$$

After some algebraic manipulations, we obtain

$$\tilde{\boldsymbol{K}}\cdot\boldsymbol{g} = \lambda(\boldsymbol{g})\cdot\tilde{\boldsymbol{J}}\cdot\boldsymbol{g}. \tag{37}$$

The matrices $\tilde{\boldsymbol{K}}$ and $\tilde{\boldsymbol{J}}$ are defined as

$$\begin{aligned}
\tilde{\boldsymbol{K}} &= \sum_{\ell=1}^{L}\sum_{k=1}^{2}\left(\prod_{\bar{k},\bar{\ell}\setminus k,\ell}\boldsymbol{g}^{\mathrm{H}}\boldsymbol{A}_{\bar{k}}^{(\bar{\ell})}\boldsymbol{g}\right)\boldsymbol{A}_k^{(\ell)} \\
\tilde{\boldsymbol{J}} &= \sum_{\ell=1}^{L}\sum_{k=1}^{2}\left(\prod_{\bar{k},\bar{\ell}\setminus k,\ell}\boldsymbol{g}^{\mathrm{H}}\boldsymbol{C}_{\bar{k}}^{(\bar{\ell})}\boldsymbol{g}\right)\boldsymbol{C}_k^{(\ell)}.
\end{aligned} \tag{38}$$

where $\bar{k},\bar{\ell}\setminus k,\ell$ stands for the whole set $\{\{\bar{k},\bar{\ell}\}|\bar{k}\in\{1,2\},\bar{\ell}\in\{1,2,\ldots,L\}\}$ excluding the condition $\{\bar{k}=k,\ \bar{\ell}=\ell\}$. Clearly, (37) shows that the optimal $\boldsymbol{g}$ must be a generalized eigenvector of the matrices $\tilde{\boldsymbol{K}}$ and $\tilde{\boldsymbol{J}}$. This is similar as in [16]. However, the bisection search of [16] can not be applied here since an increase in L will increase the number of parameters to search over and thus results in a prohibitive computational complexity. Fortunately, $\tilde{\boldsymbol{J}}$ is a positive definite matrix and thus it is invertible. Equation (37) can be reformulated into an eigenvalue problem as

$$\tilde{\boldsymbol{J}}^{-1}\tilde{\boldsymbol{K}}\cdot\boldsymbol{g} = \lambda(\boldsymbol{g})\cdot\boldsymbol{g}. \tag{39}$$

From (39) the dominant eigenvalue of $\tilde{\boldsymbol{J}}^{-1}\tilde{\boldsymbol{K}}$ will be the global optimum for (34) and the corresponding dominant eigenvector will the optimal $\boldsymbol{g}$. Although $\tilde{\boldsymbol{J}}^{-1}\tilde{\boldsymbol{K}}$ and $\lambda(\boldsymbol{g})$ are still functions of $\boldsymbol{g}$, the dominant eigenvalue and dominant eigenvector can be obtained using the power method (PM) in [4] (*Section 7.3.1*). The details for the PM are also found in Appendix C. It is worth mentioning that using PM to solve the maximization problem of the form in (34) is also observed in [11]. Although simulation results show that the PM algorithm converges, compared to ProBaSeMO it has a significantly higher computational complexity and can only be used as a benchmark.

B. Multiple Antennas at Each UT

In this section, we calculate the optimal relay amplification matrix assuming that $\boldsymbol{W}_k^{(\ell)} = \frac{\sqrt{P_k^{(\ell)}}\boldsymbol{I}_{M_{\mathrm{U}}}}{\sqrt{M_{\mathrm{U}}}}$. The achievable rate for the kth UT of the ℓth operator is

$$\begin{aligned}
R_k^{(\ell)} = \frac{1}{2}\log_2\Bigg(\Bigg|&\boldsymbol{I}_{M_{\mathrm{U}}} + \frac{P_{3-k}^{(\ell)}}{M_{\mathrm{U}}}\boldsymbol{H}_k^{(\ell)^{\mathrm{T}}}\boldsymbol{G}\boldsymbol{H}_{3-k}^{(\ell)}\boldsymbol{H}_{3-k}^{(\ell)^{\mathrm{H}}} \\
&\times\boldsymbol{G}^{\mathrm{H}}\boldsymbol{H}_k^{(\ell)^*} \\
&\cdot\Bigg(\sum_{\bar{k},\bar{\ell}\neq\ell}\frac{P_{\bar{k}}^{(\bar{\ell})}}{M_{\mathrm{U}}}\boldsymbol{H}_k^{(\ell)^{\mathrm{T}}}\boldsymbol{G}\boldsymbol{H}_{\bar{k}}^{(\bar{\ell})}\boldsymbol{H}_{\bar{k}}^{(\bar{\ell})^{\mathrm{H}}}\boldsymbol{G}^{\mathrm{H}}\boldsymbol{H}_k^{(\ell)^*} \\
&+\sigma_{\mathrm{R}}^2\boldsymbol{H}_k^{(\ell)^{\mathrm{T}}}\boldsymbol{G}\boldsymbol{G}^{\mathrm{H}}\boldsymbol{H}_k^{(\ell)^*} \\
&+{\sigma_k^{(\ell)}}^2\boldsymbol{I}_{M_{\mathrm{U}}}\Bigg)^{-1}\Bigg|\Bigg).
\end{aligned} \tag{40}$$

The sum rate maximization problem is then formulated as

$$\begin{aligned}
\max_{\boldsymbol{G}} \quad & R_{\mathrm{sum}} = \sum_{\ell=1}^{L}\sum_{k=1}^{2}R_k^{(\ell)} \\
\text{subject to} \quad & \mathbb{E}\{\|\bar{\boldsymbol{r}}\|^2\} \leq P_{\mathrm{R}}.
\end{aligned} \tag{41}$$

TABLE III
STEEPEST DESCENT METHOD FOR SUM RATE MAXIMIZATION.

Initialization step: set a random $\boldsymbol{G}$ and calculate $R_{\mathrm{sum}}^{(0)}$, maximum iteration number $N_{\max}$ and the threshold value υ.
Main step:
1: **for** $p = 1$ to $N_{\max}$ **do**
2: Calculate the steepest descent direction $\nabla R_{\mathrm{sum}}/\|\nabla R_{\mathrm{sum}}\|_{\mathrm{F}}$.
3: Choose a step size t using Armijo's Rule in (44).
4: Update $\boldsymbol{G} = \boldsymbol{G} + t\nabla R_{\mathrm{sum}}/\|\nabla R_{\mathrm{sum}}\|_{\mathrm{F}}$
5: Calculate $R_{\mathrm{sum}}^{(p)}$ with the updated $\boldsymbol{G}$.
6: **if** $\|R_{\mathrm{sum}}^{(p)} - R_{\mathrm{sum}}^{(p-1)}\| < \upsilon$ **then**
7: **break**
8: **end if**
9: **end for**

The same argument as in Section IV-A holds, i.e., the constraint has to be satisfied with equality at the optimum. Inserting the constraint into the cost function in (41), again we calculate the necessary condition for optimality. Using the tools that $d(\ln|\boldsymbol{\Gamma}|) = \mathrm{tr}\{\boldsymbol{\Gamma}^{-1}d\boldsymbol{\Gamma}\}$, $d\{\mathrm{tr}\{\boldsymbol{\Gamma}\}\} = \mathrm{tr}\{d\boldsymbol{\Gamma}\}$, the gradient of the sum rate is then obtained as:

$$\begin{aligned}\nabla R_{\mathrm{sum}} &= \frac{\partial R_{\mathrm{sum}}}{\partial \boldsymbol{G}^*} \\ &= \sum_{k,\ell} \frac{1}{2M_{\mathrm{U}}\ln 2} \\ &\quad \times \Bigg[\frac{{\sigma_k^{(\ell)}}^2}{P_{\mathrm{R}}} \mathrm{Tr}\{{\boldsymbol{\Psi}_k^{(\ell)}}^{-1} - \boldsymbol{\Psi}_{3-k}^{(\ell)^{-1}}\}\boldsymbol{G}\boldsymbol{\Omega} \\ &\qquad + \boldsymbol{H}_k^{(\ell)^*}({\boldsymbol{\Psi}_k^{(\ell)}}^{-1} - \boldsymbol{\Psi}_{3-k}^{(\ell)^{-1}}){\boldsymbol{H}_k^{(\ell)}}^{\mathrm{T}} \\ &\qquad \cdot \boldsymbol{G}(\boldsymbol{\Omega} - P_k^{(\ell)}\boldsymbol{H}_k^{(\ell)}{\boldsymbol{H}_k^{(\ell)}}^{\mathrm{H}}) \\ &\qquad + P_{3-k}^{(\ell)}\boldsymbol{H}_k^{(\ell)^*}\boldsymbol{\Psi}_{3-k}^{(\ell)^{-1}}{\boldsymbol{H}_k^{(\ell)}}^{\mathrm{H}} \\ &\qquad \times \boldsymbol{G}\boldsymbol{H}_{3-k}^{(\ell)}{\boldsymbol{H}_{3-k}^{(\ell)}}^{\mathrm{H}}\Bigg] \end{aligned} \tag{42}$$

where $\boldsymbol{\Omega}$, $\boldsymbol{\Psi}_k^{(\ell)}$, and $\boldsymbol{\Psi}_{3-k}^{(\ell)}$ are defined as

$$\begin{aligned}\boldsymbol{\Omega} &= \sum_{k,\ell} P_k^{(\ell)}\boldsymbol{H}_k^{(\ell)}{\boldsymbol{H}_k^{(\ell)}}^{\mathrm{H}} + \sigma_{\mathrm{R}}^2 M_{\mathrm{U}}\boldsymbol{I}_{M_{\mathrm{R}}} \\ \boldsymbol{\Psi}_k^{(\ell)} &= \frac{{\sigma_k^{(\ell)}}^2\mathrm{Tr}\{\boldsymbol{\Omega}\}}{M_{\mathrm{U}}P_{\mathrm{R}}}\boldsymbol{I}_{M_{\mathrm{U}}} \\ &\quad + \frac{1}{M_{\mathrm{U}}}{\boldsymbol{H}_k^{(\ell)}}^{\mathrm{T}}\boldsymbol{G}(\boldsymbol{\Omega} - P_k^{(\ell)}\boldsymbol{H}_k^{(\ell)}{\boldsymbol{H}_k^{(\ell)}}^{\mathrm{H}})\boldsymbol{G}^{\mathrm{H}}\boldsymbol{H}_k^{(\ell)^*} \\ \boldsymbol{\Psi}_{3-k}^{(\ell)} &= \boldsymbol{\Psi}_k^{(\ell)} - \frac{P_{3-k}^{(\ell)}}{M_{\mathrm{U}}}{\boldsymbol{H}_k^{(\ell)}}^{\mathrm{T}}\boldsymbol{G}\boldsymbol{H}_{3-k}^{(\ell)}{\boldsymbol{H}_{3-k}^{(\ell)}}^{\mathrm{H}}\boldsymbol{G}^{\mathrm{H}}\boldsymbol{H}_k^{(\ell)^*}. \end{aligned} \tag{43}$$

Finally, we apply the steepest descent method as in Table III to obtain $\boldsymbol{G}$. The step size t is chosen using the Armijo's Rule which provides provable convergence [2]. That is, t is calculated as $t = \beta^n$ where n is the smallest integer such that

$$\begin{aligned}&R_{\mathrm{sum}}(\boldsymbol{G} + \beta^n\nabla R_{\mathrm{sum}}) - R_{\mathrm{sum}}(\boldsymbol{G}) \\ &\qquad \leq \alpha\beta^n\mathrm{Tr}\{\nabla {R_{\mathrm{sum}}}^{\mathrm{H}}\nabla R_{\mathrm{sum}}\}. \end{aligned} \tag{44}$$

where β and α are fixed scalars between zero and one. Since the cost function in (41) is non-convex, this solution here might be merely a local minimum.

V. ACQUISITION OF CHANNEL KNOWLEDGE

The ProBaSeMO strategy requires that the relay and each UT possess channel knowledge. The relay needs to know the channels $\boldsymbol{H}_k^{(\ell)}$, $\forall k, \ell$. If a single antenna is deployed at each UT, the equivalent backward channel is needed at each UT; if multiple antennas are deployed at each UT, both the equivalent forward and backward channels are needed at each UT. In both cases, knowledge of the self-interference channel should be also obtained at each UT. In general, the equivalent backward channel can be obtained via channel estimation. If $\boldsymbol{G} = \boldsymbol{G}^{\mathrm{T}}$, the equivalent forward channel is equal to the transpose of the equivalent backward channel. Otherwise, feedback from the relay is required.

To avoid unnecessary complexity, we propose a simple extension of the least squares (LS) scheme introduced in [16] to estimate these channels. To this end, all the terminals need to transmit a sequence of $M_{\mathrm{U}} \cdot N_{\mathrm{p}}$ pilot symbols $p_{k,j}^{(\ell)}$ for $j = [1, 2, \ldots, N_{\mathrm{p}}]$. The overall training data received at the relay is then

$$\boldsymbol{B} = \sum_{\ell=1}^{L}\sum_{k=1}^{2}\boldsymbol{H}_k^{(\ell)}\boldsymbol{P}_k^{(\ell)} + \boldsymbol{N}_{\mathrm{R}} \in \mathbb{C}^{M_{\mathrm{R}} \times N_{\mathrm{p}}}, \tag{45}$$

where $\boldsymbol{N}_{\mathrm{R}}$ denotes the ZMCSCG noise matrix and the pilot matrix $\boldsymbol{P}_k^{(\ell)}$ is defined as

$$\boldsymbol{P}_k^{(\ell)} = \begin{bmatrix} p_{k,1,1}^{(\ell)} & p_{k,1,2}^{(\ell)} & \cdots & p_{k,1,N_{\mathrm{p}}}^{(\ell)} \\ p_{k,2,1}^{(\ell)} & p_{k,2,2}^{(\ell)} & \cdots & p_{k,2,N_{\mathrm{p}}}^{(\ell)} \\ \vdots & \vdots & \ddots & \vdots \\ p_{k,M_{\mathrm{U}},1}^{(\ell)} & p_{k,M_{\mathrm{U}},2}^{(\ell)} & \cdots & p_{k,M_{\mathrm{U}},N_{\mathrm{p}}}^{(\ell)} \end{bmatrix}. \tag{46}$$

Let $\boldsymbol{P} = \left[{\boldsymbol{P}_1^{(1)}}^{\mathrm{T}}, {\boldsymbol{P}_2^{(1)}}^{\mathrm{T}}, \ldots, {\boldsymbol{P}_1^{(L)}}^{\mathrm{T}}, {\boldsymbol{P}_2^{(L)}}^{\mathrm{T}}\right]^{\mathrm{T}}$ be a row-orthogonal matrix. The conventional LS estimate $\hat{\boldsymbol{H}}$ of the overall channel matrix $\boldsymbol{H}$ at the relay is obtained via

$$\hat{\boldsymbol{H}} = \boldsymbol{B} \cdot \boldsymbol{P}^{+}. \tag{47}$$

Note that (47) requires $N_{\mathrm{p}} \geq 2 \cdot L \cdot M_{\mathrm{U}}$. Let us denote the relay amplification matrix computed from the imperfect channel knowledge as $\tilde{\boldsymbol{G}}$. The relay can compute $\tilde{\boldsymbol{G}}$ as described in Section III and then transmits $\tilde{\boldsymbol{G}} \cdot \boldsymbol{B}$ to all UTs. At the kth UT of the lth operator, the received signal can be written as

$$\boldsymbol{Y}_k^{(\ell)} = \tilde{\boldsymbol{H}}_{k,k}^{(\ell)}\boldsymbol{P}_k^{(\ell)} + \tilde{\boldsymbol{H}}_{k,m}^{(\ell)}\boldsymbol{P}_m^{(\ell)} + \tilde{\boldsymbol{N}}_k^{(\ell)}, \tag{48}$$

with $m \neq k$, $m, k \in \{1, 2\}$ and $\tilde{\boldsymbol{H}}_{i,j}^{(\ell)} = {\boldsymbol{H}_i^{(\ell)}}^{\mathrm{T}}\tilde{\boldsymbol{G}}\boldsymbol{H}_j^{(\ell)}$, $\forall i, j, \ell$. The effective noise matrix is denoted by $\tilde{\boldsymbol{N}}_k^{(\ell)} = \sum_{\bar{k},\bar{\ell}\neq\ell}\boldsymbol{H}_{k,\bar{k}}^{(\ell,\bar{\ell})}\boldsymbol{P}_{\bar{k}}^{(\bar{\ell})} + \boldsymbol{G}\boldsymbol{N}_{\mathrm{R}} + \boldsymbol{N}_k^{(\ell)}$ where $\boldsymbol{N}_k^{(\ell)}$ denotes the ZMCSCG noise matrix at the UT.

Similarly, the LS estimates of the effective channels for UTs of the lth operator are given by

$$\begin{aligned}\begin{bmatrix}\hat{\boldsymbol{H}}_{1,1}^{(\ell)} & \hat{\boldsymbol{H}}_{1,2}^{(\ell)}\end{bmatrix} &= \boldsymbol{Y}_1^{(\ell)} \cdot \boldsymbol{P}^{(\ell)^+} \text{ for UT1 and} \\ \begin{bmatrix}\hat{\boldsymbol{H}}_{2,1}^{(\ell)} & \hat{\boldsymbol{H}}_{2,2}^{(\ell)}\end{bmatrix} &= \boldsymbol{Y}_2^{(\ell)} \cdot \boldsymbol{P}^{(\ell)^+} \text{ for UT2,} \end{aligned} \tag{49}$$

where $\boldsymbol{P}^{(\ell)}$ is defined as $\boldsymbol{P}^{(\ell)} = \left[\boldsymbol{P}_1^{(\ell)^{\mathrm{T}}}, \boldsymbol{P}_2^{(\ell)^{\mathrm{T}}}\right]^{\mathrm{T}}$. Here we only require that $N_{\mathrm{p}} \geq 2M_{\mathrm{U}}$. It implies that to estimate the channel at the relay requires additional training overhead.

VI. Simulation Results

In this section, the performance of the proposed algorithms are evaluated via Monte Carlo simulations. The system sum rate is calculated via (6). In the first set of simulations (Figs. 4–9), a single antenna is used at each UT and the proposed algorithms are evaluated and compared to the time-shared case as well as the algorithms in [7] and [21]. In the second set of simulations (Figs. 10–12), a similar evaluation is performed for multiple antennas at the UT. Here, "uXX" stands for the transmit strategy at each UT and "rXX" stands for the transmit strategy at the relay. In Fig. 13, the effects of CSI imperfections are evaluated and discussed. Based on the simulation results of the four ProBaSeMO approaches, i.e., {BD, RBD} & {ANOMAX, RR-ANOMAX}, the BD and the RBD strategy only differ in the low SNR regime and in general "BD ANOMAX"≤"RBD ANOMAX"< "BD RR-ANOMAX"≤"RBD RR-ANOMAX".[6] For brevity, we mainly demonstrate the performance of "BD ANOMAX" and "RBD RR-ANOMAX" in the sequel. Moreover, the time-shared case performance is labeled by "excl" which stands for exclusively. It means that the relay as well as the spectrum are used by different operators in a TDMA fashion. In particular, in the first two time slots, only the UTs of the first operator are served. In the next two time slots, the UTs of the second operator are served and so on.

The simulated MIMO flat fading channels $\boldsymbol{H}_k^{(\ell)}$ are uncorrelated Rayleigh channels except for Fig. 12. When the channel is correlated, the spatial correlation is modeled using the Kronecker model such that the channel matrix $\boldsymbol{H}_k^{(\ell)}$ is obtained from

$$\boldsymbol{H}_k^{(\ell)} = \boldsymbol{R}_{\mathrm{R}}^{\frac{1}{2}} \boldsymbol{H}_{\mathrm{w}_k}^{(\ell)} \boldsymbol{R}_k^{(\ell)^{\frac{1}{2}}}, \tag{50}$$

where $\boldsymbol{H}_{\mathrm{w}_k}^{(\ell)} \in \mathbb{C}^{M_{\mathrm{R}} \times M_{\mathrm{U}}}$ represents a spatially white unit variance flat fading MIMO channel, whereas $\boldsymbol{R}_{\mathrm{R}}$ and $\boldsymbol{R}_k^{(\ell)}$ are the spatial correlation matrices with $\mathrm{Tr}\{\boldsymbol{R}_{\mathrm{R}}\} = M_{\mathrm{R}}$ and $\mathrm{Tr}\{\boldsymbol{R}_k^{(\ell)}\} = M_{\mathrm{U}}$. The spatial correlation matrix $\boldsymbol{R}_{\mathrm{R}}$ at the relay contains ones on the main diagonal and elements with magnitude ρ_{R} and random phases on all the other positions.

The channel $\boldsymbol{H}_k^{(\ell)}$ is fixed during the training phase and the data transmission phase. The transmit power at each UT and at the relay are identical and $P_k^{(\ell)} = P_{\mathrm{R}} = 1$ W, $\forall k, \ell$. The SNR at each UT and at the relay are also identical. It is defined as $\mathrm{SNR} = \frac{1}{\sigma_{\mathrm{R}}^2} = \frac{1}{\sigma_k^{(\ell)^2}}$, $\forall k, \ell$. The weighting factor β is set to 0.5 in all simulations. All the simulation results are obtained by averaging over 1000 channel realizations.

A. Single Antenna At Each UT

Fig. 4 shows the system sum rate comparison when $M_{\mathrm{U}} = 1$ and $L = 2$. The "Optimum" and "excl Optimum" methods are based on the power method described in Section IV-A. The ProBaSeMO algorithm outperforms the time-shared approach for large values of M_{R} as well as moderate to high SNR values.

[6]"RBD ANOMAX">"BD RR-ANOMAX" in the low SNR regime. When M_{R} increases the differences become small.

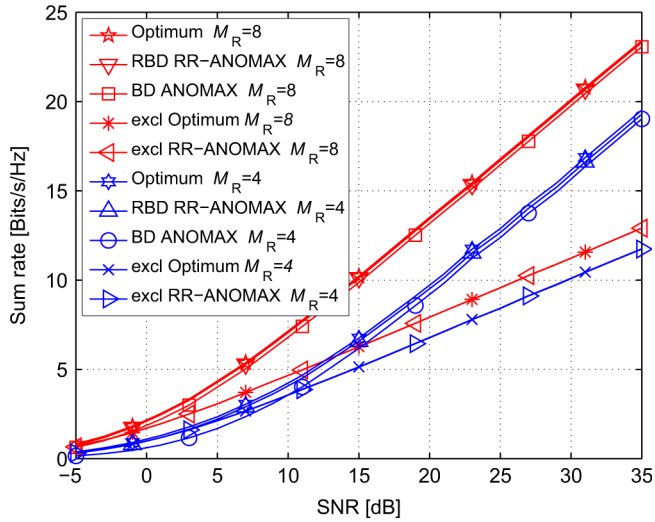

Fig. 4. Sum rate comparison of time-shared approach and ProBaSeMO approach for $M_{\mathrm{U}} = 1$ and $L = 2$.

At an SNR of 35 dB, the sharing gain is nearly two-fold due to an increased multiplexing gain. The result also implies that the ProBaSeMO algorithm coincides with the optimum when M_{R} increases.

In Fig. 5, the ProBaSeMO algorithms are compared to other techniques from the literature. The "ZF" and "MMSE" methods are the single antenna version of algorithms proposed in [7]. "YZGK10" stands for the algorithm proposed in [21]. As the result suggests, the ProBaSeMO algorithms give the best performance especially from moderate to high SNRs. When M_{R} increases, there will be sufficient degrees of freedom in the spatial dimension. Thus, non-pairing aware algorithms (ZF and MMSE) almost approach the performance of pairing aware algorithms with less than 1 dB difference. The ProBaSeMO methods can provide a gain of approximately 10 dB over the YZGK10 method at the high SNRs when $M_{\mathrm{R}} = 8$. This implies that ANOMAX offers this performance enhancement. However, all the curves have the same slope in the high SNR regime which means that they yield the same multiplexing gain.

Fig. 6 shows the sum rate as a function of the number of antennas at the relay when the SNR is 25 dB. The sharing gain of paring aware schemes (ProBaSeMO, YZGK10) as well as non-paring aware schemes (ZF and MMSE) increases as the array size at the relay increases. ProBaSeMO outperforms ZF and MMSE especially when only a few antennas are deployed at the relay, e.g., $M_{\mathrm{R}} = 3$. This is due to the fact that the ZF and the MMSE algorithms require more antennas at the relay to null the interference. It can be also seen that the time-shared approach has a better or equal performance compared to the sharing approaches when the relay has only a few antennas (e.g., 3 antennas). Again, the performance of the YZGK10 approach implies that the ANOMAX algorithm determines the gain obtained in the ProBaSeMO schemes.

Fig. 7 demonstrates the system loading capability for both high SNR (25 dB) and low SNR (5 dB) when the relay has 20 antennas. It shows that increasing the number of operators which share the spectrum and the relay will increase the sharing gain.

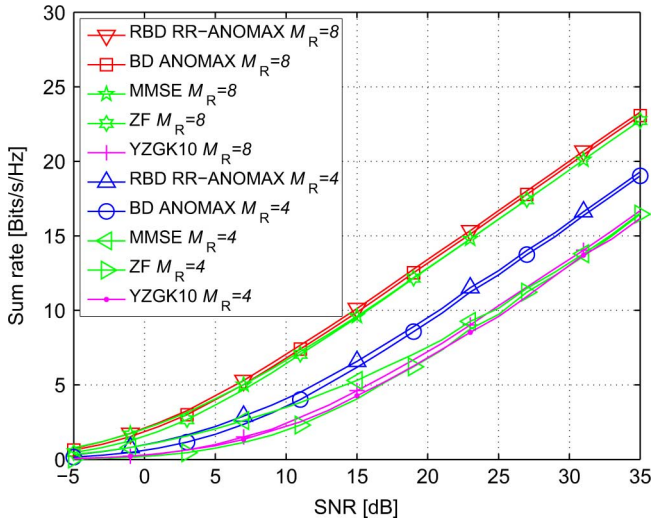

Fig. 5. Sum rate comparison of different multi-operator TWR approaches for $M_{\mathrm{U}} = 1$ and $L = 2$.

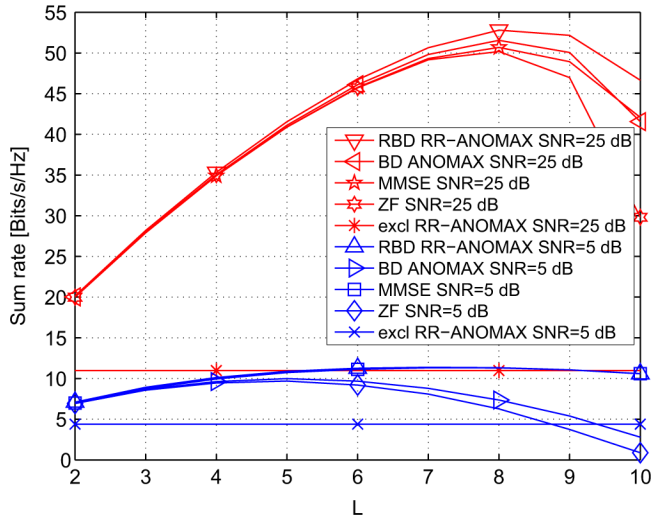

Fig. 7. Sum rate comparison of different multi-operator TWR approaches for $M_{\mathrm{U}} = 1$ and $M_{\mathrm{R}} = 20$.

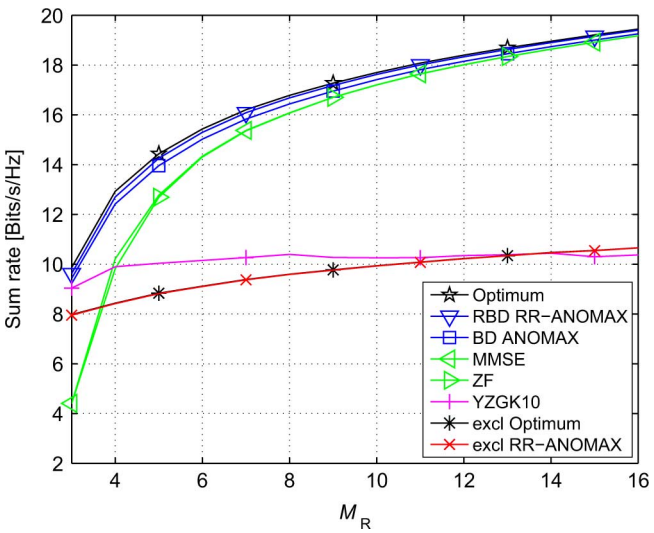

Fig. 6. Sum rate comparison of different multi-operator TWR approaches for $M_{\mathrm{U}} = 1$, SNR $= 25$ dB and $L = 2$.

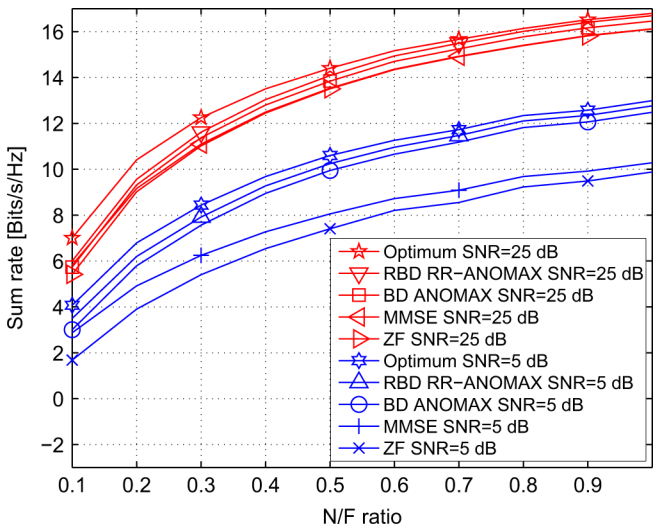

Fig. 8. Effects of path loss of different multi-operator TWR approaches for $M_{\mathrm{R}} = 8$, $M_{\mathrm{U}} = 1$ and $L = 2$.

However, due to the dimensionality constraint of the SDMA based appraches, there is a turning point after which increasing number of operators will decrease the system sum rate.

Fig. 8 demonstrates the effects of path loss on the sum rate performance for $M_{\mathrm{R}} = 8$. The path loss model $P_L = 20\log_{10}(d_k^{(\ell)})$ is applied where $d_k^{(\ell)}$ is the normalized distance between the relay and the UT. We further assume a symmetric system model, i.e., $d_1^{(\ell)} = d_1$ and $d_2^{(\ell)} = d_2\ \forall \ell$. The near-far (N/F) ratio is defined as $\frac{d_2}{d_1}$. It can be seen that the suboptimal algorithms suffer more loss when the ratio is smaller that 0.5.

Fig. 9 illustrates the uncoded system BER performance of different algorithms. Uncoded system BER is defined as the average over all UTs' uncoded BERs. Among all algorithms, RBD RR-ANOMAX provides the best performance. Not surprisingly, the RBD ANOMAX solution has a slightly worse performance than BD ANOMAX. There are two reasons. First, the low rank nature of ANOMAX will cause more bit errors in some data streams and the worst data stream dominates the BER performance. Second, compared to the BD solution, the singular value profile of the RBD solution is more imbalanced [20]. This will result in a worse decoding situation. Thus, substituting ANOMAX with RR-ANOMAX provides a better BER performance. Another method for improving the RBD ANOMAX performance is to use the power loading method in [20]. However, it requires a significantly higher computational complexity.

B. Two Antennas at Each UT

Fig. 10 shows the comparison of different transmission strategies when each UT has 2 antennas. Three precoding approaches, namely, "uWF (water-filling algorithm in Section III-D)", "uDET" (dominant eigenmode transmission in Section III-D) and "uJou2010" (dominant eigen beamforming in [7] which uses a different effective channel from "uDET"), are compared in this simulation. "rStDe" is the steepest descent method in Section IV-B. Compared to the time-shared approach, the

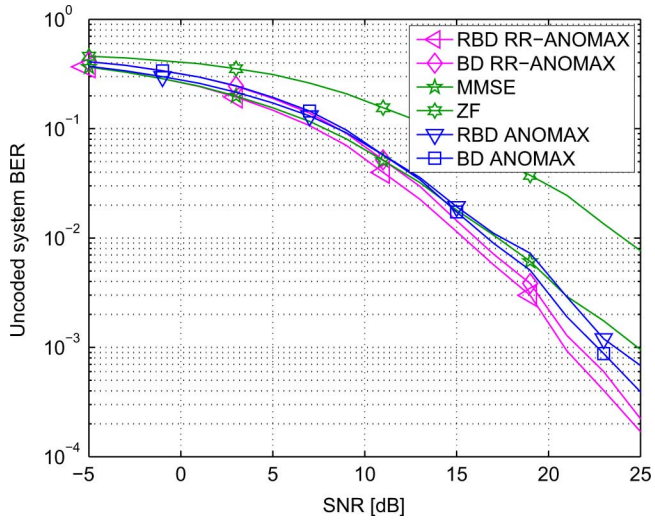

Fig. 9. Uncoded system BER comparison of different multi-operator TWR approaches for QPSK modulation, $M_{\mathrm{U}} = 1$, $M_{\mathrm{R}} = 4$ and $L = 2$.

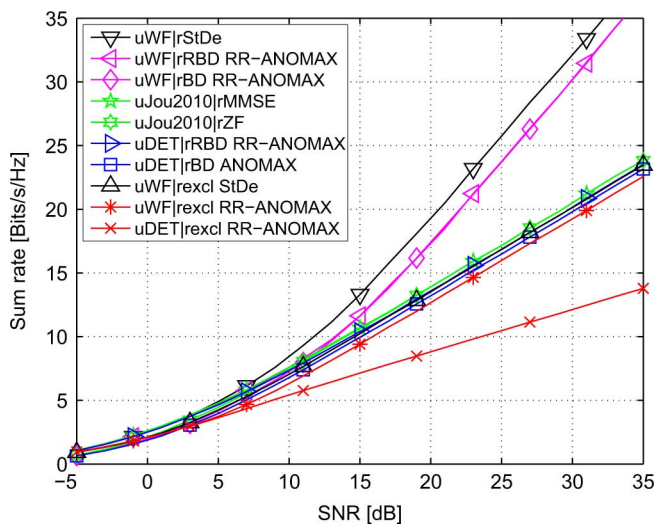

Fig. 10. Sum rate comparison of different multi-operator TWR approaches for $M_{\mathrm{U}} = 2$, $M_{\mathrm{R}} = 8$ and $L = 2$.

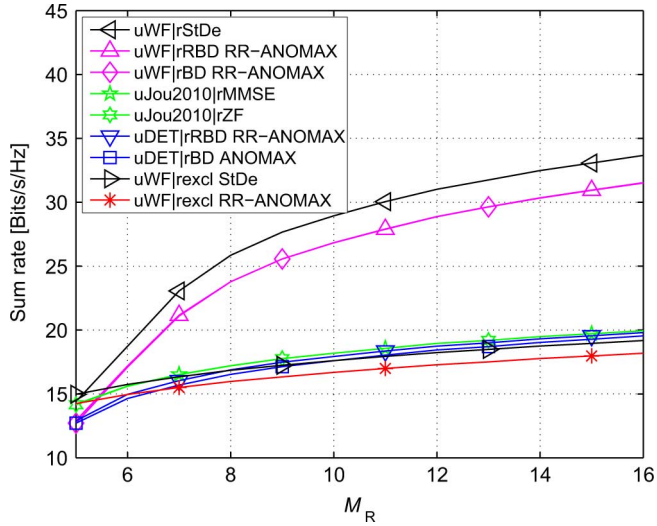

Fig. 11. Sum rate comparison of different multi-operator TWR approaches for $M_{\mathrm{U}} = 2$, SNR $= 25$ dB and $L = 2$.

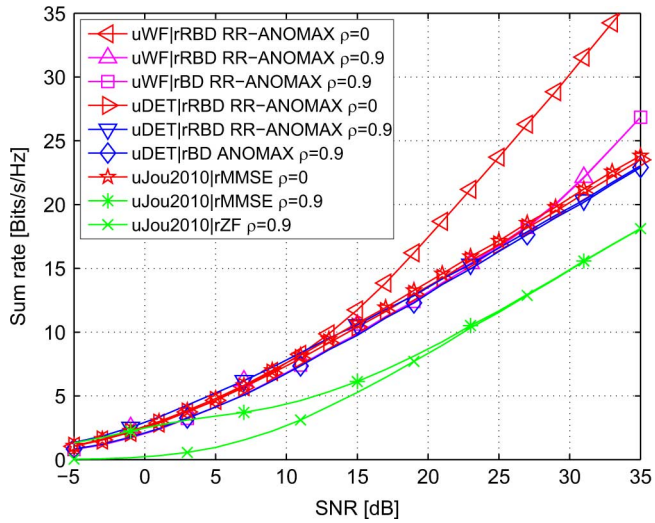

Fig. 12. Sum rate comparison of different approaches for $M_{\mathrm{U}} = 2$, $M_{\mathrm{R}} = 8$, and $L = 2$ when $\rho_{\mathrm{R}} = 0.9$.

ProBaSeMO approaches obtain an almost two-fold sharing gain in terms of the sum rate at an SNR of 35 dB due to the increased slope of the curves (increased spatial multiplexing gain). Moreover, the ProBaSeMO approaches have achieved the same multiplexing gain as the steepest descent method but with much less computational complexity.

In Fig. 11, the sum rate performance is shown as a function of the number of antennas at the relay at high SNR (25 dB). As M_{R} increases, the slope of ProBaSeMO is higher compared to the time-shared approaches. This means that larger sharing gains are obtained when the relay has more antennas. However, when the relay has only 5 antennas, the time-shared approach slightly outperforms ProBaSeMO because the SDMA approach sacrifices the available degrees of freedom. Nevertheless, the ProBaSeMO scheme achieves the same multiplexing gain as the steepest descent method.

Fig. 12 demonstrates the sum rate comparison of different transmission strategies when spatial correlation exists at the relay, i.e., $\rho_{\mathrm{R}} = 0.9$. The ProBaSeMO algorithms with single stream transmission are robust against this kind of correlation while multiple stream transmission suffers from spatial correlation. However, the ZF and MMSE methods have a significant degradation of the performance even in the case of single stream transmission.

C. CSI Imperfections

In Fig. 13, we show the effects of the CSI imperfection on the system spectral efficiency when each UT has 2 antennas and the relay has 8 antennas. Each UT transmits 8 pilot symbols. The spectral efficiency is defined as (Number of correctly received packets $\times$ Number of bits per packet/Total transmission time). "LS r+u" denotes that the LS channel estimation method in Section V is applied at all nodes while "pCSI" stands for perfect CSI. As can be seen, the ProBaSeMO approaches are not sensitive (in this simulation less than 1 dB) to channel estimation errors. Note that we have not compared to the techniques in

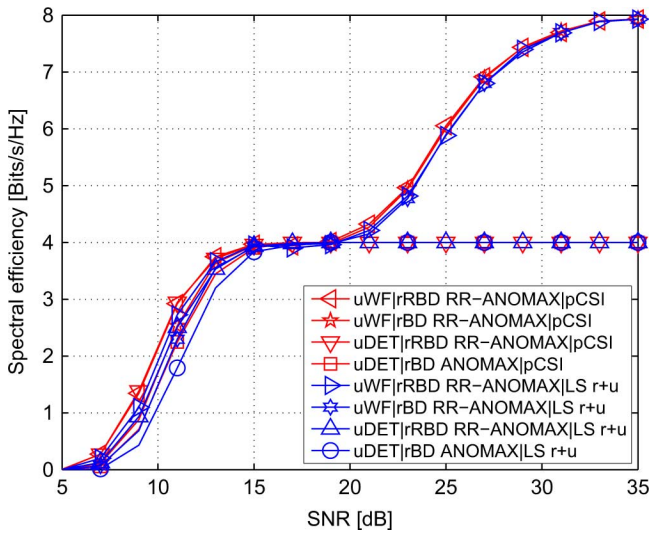

Fig. 13. System spectral efficiency comparison of different approaches for QPSK modulation, $M_{\mathrm{U}} = 2$, $M_{\mathrm{R}} = 8$ and $L = 2$.

[7] since each UT needs to acquire $\boldsymbol{H}_k^{(\ell)}$ and the CSI acquisition method is not specified in [7].

VII. Conclusions

In this paper, we investigate a relay sharing model where the relay and the spectrum are shared between multiple operators. We demonstrate that all operators can serve their users by using multiple antennas at the relay via the proposed projection based separation of multiple operators (ProBaSeMO) strategy inspired by the BD and RBD MU-MIMO precoding schemes. This ProBaSeMO strategy can be applied for both single- and multi-antenna at the UTs. Transmit- and receive- strategies for both single-stream and multi-stream transmission are also proposed. In a two-operator case, it can provide a significant sharing gain with many antennas at the relay or in the high SNR regime regardless of single stream transmission or multiple stream transmission at the UTs. For a fixed number of antennas at the relay, a higher sharing gain can be obtained if the number of operators increases. The ProBaSeMO strategy has a smaller dimensionality constraint compared to the non-pairing aware methods in [7]. It also outperforms the algorithms in [7] and [21] in terms of sum rate. Moreover, it is more robust with respect to the channel correlation at the relay compared to the schemes in [7]. To obtain the instantaneous CSI, we propose a training-based LS channel estimation scheme. It is verified that the ProBaSeMO strategy is not sensitive to the CSI imperfection.

Appendix A
Derivation of RBD in the MAC Phase

Recall the cost function in (16), it can be further expanded as

$$\begin{aligned}\boldsymbol{G}_{\mathrm{R}} &= \min_{\boldsymbol{G}_{\mathrm{R}}} \mathbb{E}\left\{ \sum_{l=1}^{L} \left\| \boldsymbol{G}_{\mathrm{R}}^{(\ell)} \tilde{\boldsymbol{H}}^{(l)} \tilde{\boldsymbol{x}}^{(\ell)} \right\|^2 + \sum_{l=1}^{L} \left\| \boldsymbol{G}_{\mathrm{R}}^{(\ell)} \boldsymbol{n}_{\mathrm{R}} \right\|^2 \right\} \\ &= \min_{\boldsymbol{G}_{\mathrm{R}}} \mathbb{E}\left\{ \sum_{l=1}^{L} \left(\mathrm{Tr}\left\{ \boldsymbol{G}_{\mathrm{R}}^{(\ell)} \tilde{\boldsymbol{H}}^{(l)} \tilde{\boldsymbol{x}}^{(\ell)} \tilde{\boldsymbol{x}}^{(\ell)^{\mathrm{H}}} \tilde{\boldsymbol{H}}^{(\ell)^{\mathrm{H}}} \boldsymbol{G}_{\mathrm{R}}^{(\ell)^{\mathrm{H}}} \right.\right.\right. \\ &\qquad \left.\left.\left. + \boldsymbol{G}_{\mathrm{R}}^{(\ell)} \boldsymbol{n}_{\mathrm{R}} \boldsymbol{n}_{\mathrm{R}}^{\mathrm{H}} \boldsymbol{G}_{\mathrm{R}}^{(\ell)^{\mathrm{H}}} \right\} \right) \right\}. \end{aligned} \tag{51}$$

Using $\mathbb{E}\{\tilde{\boldsymbol{x}}^{(\ell)} \tilde{\boldsymbol{x}}^{(\ell)^{\mathrm{H}}}\} = P_k^{(\ell)} \boldsymbol{I}_{2(L-1)M_{\mathrm{U}}}$, we obtain

$$\begin{aligned} &\min_{\boldsymbol{G}_{\mathrm{R}}} \mathbb{E}\left\{ \sum_{l=1}^{L} \left(\mathrm{Tr}\left\{ \boldsymbol{G}_{\mathrm{R}}^{(\ell)} \tilde{\boldsymbol{H}}^{(l)} \tilde{\boldsymbol{x}}^{(\ell)} \tilde{\boldsymbol{x}}^{(\ell)^{\mathrm{H}}} \tilde{\boldsymbol{H}}^{(\ell)^{\mathrm{H}}} \boldsymbol{G}_{\mathrm{R}}^{(\ell)^{\mathrm{H}}} \right.\right.\right. \\ &\qquad \left.\left.\left. + \boldsymbol{G}_{\mathrm{R}}^{(\ell)} \boldsymbol{n}_{\mathrm{R}} \boldsymbol{n}_{\mathrm{R}}^{\mathrm{H}} \boldsymbol{G}_{\mathrm{R}}^{(\ell)^{\mathrm{H}}} \right\} \right) \right\} \\ &= \min_{\boldsymbol{G}_{\mathrm{R}}} \left\{ \sum_{l=1}^{L} \left(\mathrm{Tr}\left\{ \boldsymbol{G}_{\mathrm{R}}^{(\ell)} \left(\frac{P_k^{(\ell)}}{M_{\mathrm{U}}} \tilde{\boldsymbol{H}}^{(\ell)} \tilde{\boldsymbol{H}}^{(\ell)^{\mathrm{H}}} + \sigma_{\mathrm{R}}^2 \boldsymbol{I}_{M_{\mathrm{R}}} \right) \right.\right.\right. \\ &\qquad \left.\left.\left. \times \boldsymbol{G}_{\mathrm{R}}^{(\ell)^{\mathrm{H}}} \right\} \right) \right\} \\ &= \min_{\boldsymbol{G}_{\mathrm{R}}} \left\{ \sum_{l=1}^{L} \left(\mathrm{Tr}\left\{ \boldsymbol{G}_{\mathrm{R}}^{(\ell)} \tilde{\boldsymbol{U}}^{(\ell)} \left(\frac{P_k^{(\ell)}}{M_{\mathrm{U}}} \tilde{\boldsymbol{\Sigma}}^{(\ell)} \tilde{\boldsymbol{\Sigma}}^{(\ell)^{\mathrm{H}}} + \sigma_{\mathrm{R}}^2 \boldsymbol{I}_{M_{\mathrm{R}}} \right) \right.\right.\right. \\ &\qquad \left.\left.\left. \times \tilde{\boldsymbol{U}}^{(\ell)^{\mathrm{H}}} \boldsymbol{G}_{\mathrm{R}}^{(\ell)^{\mathrm{H}}} \right\} \right) \right\}. \end{aligned} \tag{52}$$

According to [20], the expression in (52) is minimized by choosing $\boldsymbol{G}_{\mathrm{R}}^{(\ell)} = \boldsymbol{D}^{(\ell)} \boldsymbol{T}^{(\ell)}$ and $\boldsymbol{T}^{(\ell)} = \tilde{\boldsymbol{U}}^{(\ell)^{\mathrm{H}}}$. Then (52) reduces to

$$\min_{\boldsymbol{D}^{(\ell)}} \left\{ \sum_{l=1}^{L} \left(\mathrm{Tr}\left\{ \left(\frac{P_k^{(\ell)}}{M_{\mathrm{U}}} \tilde{\boldsymbol{\Sigma}}^{(\ell)} \tilde{\boldsymbol{\Sigma}}^{(\ell)^{\mathrm{H}}} + \sigma_{\mathrm{R}}^2 \boldsymbol{I}_{M_{\mathrm{R}}} \right) \boldsymbol{D}^{(\ell)^2} \right\} \right) \right\} \tag{53}$$

where the matrices $\boldsymbol{D}^{(\ell)}$ have to be positive definite in order to find a nontrivial solution to (53) [20]. Using the results from [20], the final solution to (52) is given by

$$\boldsymbol{G}_{\mathrm{R}}^{(\ell)} = \left(\frac{P_k^{(\ell)}}{M_{\mathrm{U}}} \tilde{\boldsymbol{\Sigma}}^{(\ell)} \tilde{\boldsymbol{\Sigma}}^{(\ell)^{\mathrm{H}}} + \sigma_{\mathrm{R}}^2 \boldsymbol{I}_{M_{\mathrm{R}}} \right)^{-\frac{1}{2}} \tilde{\boldsymbol{U}}^{(\ell)^{\mathrm{H}}}. \tag{54}$$

Note that an additional constraint $\mathbb{E}\{\|\boldsymbol{G}_{\mathrm{R}}^{(\ell)} \boldsymbol{H}^{(\ell)} \boldsymbol{x}^{(\ell)}\|^2\} = \sum_{k=1}^{2} P_k^{(\ell)}$ can be imposed on $\boldsymbol{G}_{\mathrm{R}}^{(\ell)}$ so that after applying $\boldsymbol{G}_{\mathrm{R}}$ the level of the received signal power is normalized to the transmit power. However, since the AF relay does not decode the signal and the scaling with regard to the transmit power is handled via γ_0 we will not apply the normalization here.

Appendix B
Calculation of the Precoding and Ddecoding Matrices in the Presence of Colored Noise

Taking the first UT of the ℓth operator as an example and recalling the signal model in (21), the received signal of the first UT after subtracting the self-interference is:

$$\tilde{\boldsymbol{y}}_1^{(\ell)} = \boldsymbol{H}_{1,2}^{(\ell)} \boldsymbol{x}_2^{(\ell)} + \tilde{\boldsymbol{n}}_1^{(\ell)}. \tag{55}$$

Define the covariance matrix of the colored noise as $\boldsymbol{R}_{nn} = \mathbb{E}\{\tilde{\boldsymbol{n}}_1^{(\ell)} \tilde{\boldsymbol{n}}_1^{(\ell)^{\mathrm{H}}}\}$. To whiten the colored noise, we compute the

EVD as $\boldsymbol{R}_{nn} = \boldsymbol{U}_n \boldsymbol{\Sigma}_n \boldsymbol{U}_n^{\mathrm{H}}$. Then the pre-whitening filter is chosen as:

$$\boldsymbol{R}_{\mathrm{whiten}} = \boldsymbol{\Sigma}_n^{-\frac{1}{2}} \boldsymbol{U}_n^{\mathrm{H}}. \tag{56}$$

Pre-multiplying (55) by $\boldsymbol{R}_{\mathrm{whiten}}$, the SVD of the effective channel $\boldsymbol{H}_{1,2}^{(\mathrm{eff})} = \boldsymbol{R}_{\mathrm{whiten}} \boldsymbol{H}_{1,2}^{(\ell)}$ can be obtained by:

$$\boldsymbol{H}_{1,2}^{(\mathrm{eff})} = \boldsymbol{U}_{1,2}^{(\mathrm{eff})} \boldsymbol{\Sigma}_{1,2}^{(\mathrm{eff})} \boldsymbol{V}_{1,2}^{(\mathrm{eff})^{\mathrm{H}}}. \tag{57}$$

When DET is applied, the transmit beamforming vector $\boldsymbol{W}_2^{(\ell)} = \boldsymbol{w}_2^{(\ell)}$ and receive beamforming vector $\boldsymbol{F}_1^{(\ell)} = \boldsymbol{f}_1^{(\ell)}$ are selected as the first column of $\boldsymbol{V}_{1,2}^{(\mathrm{eff})}$ and the conjugate transpose of the first column of $\boldsymbol{U}_{1,2}^{(\mathrm{eff})}$, respectively.

When spatial multiplexing is applied, a new matrix $\boldsymbol{\Sigma}_{1,2}^{(\mathrm{wf})}$ is obtained by adjusting singular values in $\boldsymbol{\Sigma}_{1,2}^{(\mathrm{eff})}$ using the water-filling algorithm in [12]. The transmit covariance matrix is given by:

$$\boldsymbol{R}_{\boldsymbol{x}_2^{(\ell)}\boldsymbol{x}_2^{(\ell)}} = \boldsymbol{V}_{1,2}^{(\mathrm{eff})} \boldsymbol{\Sigma}_{1,2}^{(\mathrm{wf})} \boldsymbol{V}_{1,2}^{(\mathrm{eff})^{\mathrm{H}}}. \tag{58}$$

with $\boldsymbol{W}_2^{(\ell)} = \boldsymbol{V}_{1,2}^{(\mathrm{eff})} \boldsymbol{\Sigma}_{1,2}^{(\mathrm{wf})^{\frac{1}{2}}}$. The decoding matrix can be chosen as $\boldsymbol{F}_1^{(\ell)} = \boldsymbol{U}_{1,2}^{(\mathrm{eff})^{\mathrm{H}}} \boldsymbol{R}_{\mathrm{whiten}}$.

Appendix C
Sum Rate Maximization Details for Single Antenna Case

Using $\mathrm{Tr}\{\boldsymbol{\Gamma}\boldsymbol{\zeta}\} = \mathrm{Tr}\{\boldsymbol{\zeta}\boldsymbol{\Gamma}\}$ and $\mathrm{vec}\{\boldsymbol{\Gamma}\boldsymbol{X}\boldsymbol{\zeta}\} = (\boldsymbol{\zeta}^{\mathrm{T}} \otimes \boldsymbol{\Gamma})\mathrm{vec}\{\boldsymbol{X}\}$, the numerator of (28), i.e., the signal power, is further expanded as

$$\begin{aligned}
&\mathbb{E}\left\{ |\boldsymbol{h}_k^{(\ell)^{\mathrm{T}}} \boldsymbol{G} \boldsymbol{h}_{3-k}^{(\ell)} x_{3-k}^{(\ell)}|^2 \right\} \\
&= P_k^{(\ell)} \mathrm{Tr}\left\{ \boldsymbol{h}_k^{(\ell)^{\mathrm{T}}} \boldsymbol{G} \boldsymbol{h}_{3-k}^{(\ell)} \left(\boldsymbol{h}_k^{(\ell)^{\mathrm{T}}} \boldsymbol{G} \boldsymbol{h}_{3-k}^{(\ell)} \right)^{\mathrm{H}} \right\} \\
&= P_k^{(\ell)} \mathrm{Tr}\left\{ (\boldsymbol{h}_{3-k}^{(\ell)^{\mathrm{T}}} \otimes \boldsymbol{h}_k^{(\ell)^{\mathrm{T}}}) \boldsymbol{g} \left((\boldsymbol{h}_{3-k}^{(\ell)^{\mathrm{T}}} \otimes \boldsymbol{h}_k^{(\ell)^{\mathrm{T}}}) \boldsymbol{g} \right)^{\mathrm{H}} \right\} \\
&= \boldsymbol{g}^{\mathrm{H}} \underbrace{\left(P_k^{(\ell)} (\boldsymbol{h}_{3-k}^{(\ell)^{\mathrm{T}}} \otimes \boldsymbol{h}_k^{(\ell)^{\mathrm{T}}})^{\mathrm{H}} (\boldsymbol{h}_{3-k}^{(\ell)^{\mathrm{T}}} \otimes \boldsymbol{h}_k^{(\ell)^{\mathrm{T}}}) \right)}_{\boldsymbol{\Phi}_k^{(\ell)}} \boldsymbol{g}.
\end{aligned} \tag{59}$$

Noticing that the interference term in (28) and the transmitted symbols are independently distributed with zero mean, the interference term can be calculated as

$$\begin{aligned}
&\mathbb{E}\left\{ \left| \sum_{\bar{k},\bar{\ell}\neq\ell} \boldsymbol{h}_k^{(\ell)^{\mathrm{T}}} \boldsymbol{G} \boldsymbol{h}_{\bar{k}}^{(\bar{\ell})} \boldsymbol{x}_{\bar{k}}^{(\bar{\ell})} \right|^2 \right\} \\
&\quad = \boldsymbol{g}^{\mathrm{H}} \underbrace{\left(\sum_{\bar{k},\bar{\ell}\neq\ell} P_{\bar{k}}^{(\bar{\ell})} (\boldsymbol{h}_{\bar{k}}^{(\bar{\ell})^{\mathrm{T}}} \otimes \boldsymbol{h}_k^{(\ell)^{\mathrm{T}}})^{\mathrm{H}} (\boldsymbol{h}_{\bar{k}}^{(\bar{\ell})^{\mathrm{T}}} \otimes \boldsymbol{h}_k^{(\ell)^{\mathrm{T}}}) \right)}_{\boldsymbol{\Upsilon}_k^{(\ell)}} \boldsymbol{g}.
\end{aligned}$$

TABLE IV
Power Method for Sum Rate Maximization

Initialization step: set a random $\boldsymbol{g}^{(0)}$,
maximum iteration number $N_{\max}$ and the threshold value υ.

Main step:
1: **for** $p = 1$ to $N_{\max}$ **do**
2: Calculate $\boldsymbol{\Psi}^{(p-1)} = (\tilde{\boldsymbol{J}}^{-1}\tilde{\boldsymbol{K}})^{(p-1)}$ using $\boldsymbol{g}^{(p-1)}$.
3: $\boldsymbol{z}^{(p)} = \boldsymbol{\Psi}^{(p-1)} \boldsymbol{g}^{(p-1)}$
4: $\boldsymbol{g}^{(p)} = \boldsymbol{z}^{(p)} / \|\boldsymbol{z}^{(p)}\|$
5: **if** $\|\boldsymbol{g}^{(p)} - \boldsymbol{g}^{(p-1)}\| < \upsilon$ **then**
6: **break**
7: **end if**
8: **end for**

Finally, the forwarded noise term is calculated as

$$\begin{aligned}
&\mathbb{E}\left\{ |\boldsymbol{h}_k^{(\ell)^{\mathrm{T}}} \boldsymbol{G} \boldsymbol{n}_{\mathrm{R}}|^2 \right\} \\
&= \sigma_{\mathrm{R}}^2 \boldsymbol{h}_k^{(\ell)^{\mathrm{T}}} \boldsymbol{G} \boldsymbol{G}^{\mathrm{H}} \boldsymbol{h}_k^{(\ell)^*} \\
&= \sigma_{\mathrm{R}}^2 \mathrm{vec}\{\boldsymbol{h}_k^{(\ell)^{\mathrm{T}}} \boldsymbol{G}\}^{\mathrm{H}} \mathrm{vec}\{\boldsymbol{h}_k^{(\ell)^{\mathrm{T}}} \boldsymbol{G}\} \\
&= \sigma_{\mathrm{R}}^2 ((\boldsymbol{I}_{M_{\mathrm{R}}} \otimes \boldsymbol{h}_k^{(\ell)^{\mathrm{T}}}) \cdot \boldsymbol{g})^{\mathrm{H}} (\boldsymbol{I}_{M_{\mathrm{R}}} \otimes \boldsymbol{h}_k^{(\ell)^{\mathrm{T}}}) \cdot \boldsymbol{g} \\
&= \boldsymbol{g}^{\mathrm{H}} \underbrace{\left(\sigma_{\mathrm{R}}^2 (\boldsymbol{I}_{M_{\mathrm{R}}} \otimes (\boldsymbol{h}_k^{(\ell)} \boldsymbol{h}_k^{(\ell)^{\mathrm{H}}})^{\mathrm{T}}) \right)}_{\boldsymbol{\Delta}_k^{(\ell)}} \boldsymbol{g}.
\end{aligned} \tag{60}$$

The power method for solving (39) is in Table IV.

Acknowledgment

The authors acknowledge fruitful discussions with Prof. Sergiy A. Vorobyov and contributions from our student Seyed Omid Taghizadeh Motlagh to Section IV-B.

References

[1] Mobile Infrastructure Sharing GSM Association, 2008 [Online]. Available: http://www.gsmworld.com/documents/gsma.pdf
[2] D. P. Bertsekas, *Nonlinear Programming*. New York: Athena Scientific, 1995.
[3] S. F.-Dehkordy, S. Shahbazpanahi, and S. Gazor, "Multiple peer-to-peer communications using a network of relays," *IEEE Trans. Signal Process.*, vol. 57, pp. 3053–3062, Aug. 2009.
[4] G. H. Golub and C. F. V. Loan, *Matrix Computations*. Baltimore, MD: The Johns Hopkins Univ. Press, 1996.
[5] V. H.-Nassab, S. Shahbazpanahi, and A. Grami, "Joint receive-transmit beamforming for multi-antenna relaying schemes," *IEEE Trans. Signal Process.*, vol. 58, pp. 4966–4972, Sep. 2010.
[6] E. Jorswieck, L. Badia, T. Fahldieck, D. Gesbert, S. Gustafsson, M. Haardt, K. Ho, E. Karipidis, A. Kortke, E. Larsson, H. Mark, M. Nawrocki, V. Palestini, R. Piesiewicz, P. Priotti, F. Roemer, M. Schubert, J. Sykora, P. Trommelen, B. van den Ende, and M. Zorzi, "Resource sharing in wireless networks: The Saphyre approach," in *Proc. Future Netw. Mobile Summit*, Florence, Italy, Jun. 2010.
[7] J. Joung and A. H. Sayed, "Multi-user two-way amplify-and-forward relay processing and power control methods for beamforming systems," *IEEE Trans. Signal Process.*, vol. 58, pp. 1833–1846, Mar. 2010.
[8] B. Khoshnevis, W. Yu, and R. Adve, "Grassmannian beamforming for MIMO amplify-and-forward relaying," *IEEE J. Sel. Areas Commun.*, vol. 26, pp. 1397–1407, Oct. 2008.
[9] E. G. Larsson, E. A. Jorswieck, J. Lindblom, and R. Mochaourab, "Game theory and the flat-fading Gaussian interference channel," *Signal Processing Mag.*, Sep. 2009.
[10] K.-J. Lee, K. W. Lee, H. Sung, and I. Lee, "Sum-rate maximization for two-way MIMO amplify-and-forward relaying systems," in *Proc. IEEE Veh. Technol. Conf. (VTC)*, Barcelona, Spain, Apr. 2009.
[11] N. Lee, H. J. Yang, and J. Chun, "Achievable sum-rate maximizing AF relay beamforming scheme in two-way relay channels," in *Proc. IEEE Int. Conf. on Commun. (ICC 2008)*, Beijing, China, May 2008.

[12] A. Paulraj, R. Nabar, and D. Gore, *Introduction to Space-Time Wireless Communications*. Cambridge, U.K.: Cambridge Univ. Press, 2003.
[13] B. Rankov and A. Wittneben, "Spectral efficient protocols for half-duplex fading relay channels," *IEEE J. Sel. Areas Commun.*, vol. 25, pp. 379–389, Feb. 2007.
[14] F. Roemer and M. Haardt, "Algebraic norm-maximizing (ANOMAX) transmit strategy for two-way relaying with MIMO amplify and forward relays," *IEEE Signal Process. Lett.*, vol. 16, Oct. 2009.
[15] F. Roemer and M. Haardt, "A low-complexity relay transmit strategy for two-way relaying with MIMO amplify and forward relays," in *Proc. IEEE Int. Conf. Acoust., Speech Signal Process. (ICASSP 2010)*, Dallas, TX, Mar. 2010.
[16] F. Roemer and M. Haardt, "Sum-rate maximization in two-way relaying systems with MIMO amplify and forward relays via generalized eigenvectors," in *Proc. 18th Eur. Signal Process. Conf. (EUSIPCO 2010)*, Aalborg, Denmark, Aug. 2010.
[17] F. Roemer, J. Zhang, M. Haardt, and E. Jorswieck, "Spectrum and infrastructure sharing in wireless networks: A case study with relay-assisted communications," in *Proc. Future Netw. Mobile Summit*, Florence, Italy, Jun. 2010.
[18] B. Song and M. Haardt, "Achievable throughput approximation for RBD precoding at high SNRs," in *Proc. IEEE Int. Conf. on Acoust., Speech, Signal Process. (ICASSP)*, Taipei, Taiwan, Apr. 2009.
[19] Q. H. Spencer, A. L. Swindlehurst, and M. Haardt, "Zero-forcing methods for downlink spatial multiplexing in multi-user MIMO channels," *IEEE Trans. Signal Process.*, vol. 52, pp. 461–471, Feb. 2004.
[20] V. Stankovic and M. Haardt, "Generalized design of multi-user MIMO precoding matrices," *IEEE Trans. Wireless Commun.*, vol. 7, pp. 953–961, Mar. 2008.
[21] E. Yilmaz, R. Zakhour, D. Gesbert, and R. Knopp, "Multi-pair two-way relay channel with multiple antenna relay station," in *Proc. IEEE Int. Conf. on Commun. (ICC 2010)*, Cape Town, South Africa, May 2010.
[22] R. Zhang, Y. Liang, C. C. Chai, and S. Cui, "Optimal beamforming for two-way multi-antenna relay channel with analogue network coding," *IEEE J. Sel. Areas Commun.*, vol. 27, pp. 699–712, Jun. 2009.

Jianshu Zhang (S'09) received the B.E. degree in computer science from Sichuan University, Chengdu, China, the M.B.A. degree in global management, and the M.Sc. degree in electrical engineering from Bremen University of Applied Sciences, Bremen, Germany, and another M.Sc. degree in computer science and communications engineering from the University of Duisburg-Essen, Duisburg, Germany, in 2003, 2004, 2006, and 2009, respectively.

Since January 2010, he has been a Research Assistant in the Communications Research Laboratory, Ilmenau University of Technology. His research interests include multidimensional signal processing, optimization theory as well as multi-user MIMO precoding and relaying.

Florian Roemer (S'04) has studied computer engineering at Ilmenau University of Technology, Germany, and McMaster University, Canada. He received the Diplom-Ingenieur (M.S.) degree with a major in communications engineering in October 2006. For his diploma thesis he received the Siemens Communications Academic Award 2006.

Since December 2006, he has been a Research Assistant with the Communications Research Laboratory, Ilmenau University of Technology. His research interests include multidimensional signal processing, high-resolution parameter estimation, as well as multi-user MIMO precoding and relaying.

Martin Haardt (S'90–M'98–SM'99) studied electrical engineering at the Ruhr-University Bochum, Germany, and at Purdue University, West Lafayette, IN. He received the Diplom-Ingenieur (M.S.) degree from the Ruhr-University Bochum in 1991 and the Doktor-Ingenieur (Ph.D.) degree from Munich University of Technology, Germany, in 1996.

In 1997 he joined Siemens Mobile Networks, Munich, where he was responsible for strategic research for third generation mobile radio systems. From 1998 to 2001, he was the Director for International Projects and University Cooperations in the mobile infrastructure business of Siemens in Munich, where his work focused on mobile communications beyond the third generation. During his time at Siemens, he also taught in the international Master of Science in Communications Engineering program at the Munich University of Technology. He has been a Full Professor in the Department of Electrical Engineering and Information Technology and Head of the Communications Research Laboratory, Ilmenau University of Technology, Germany, since 2001. His research interests include wireless communications, array signal processing, high-resolution parameter estimation, as well as numerical linear and multilinear algebra.

Dr. Haardt received the 2009 Best Paper Award from the IEEE Signal Processing Society, the Vodafone (formerly Mannesmann Mobilfunk) Innovations-Award for outstanding research in mobile communications, the ITG best paper award from the Association of Electrical Engineering, Electronics, and Information Technology (VDE), and the Rohde & Schwarz Outstanding Dissertation Award. In fall 2006 and fall 2007, he was a visiting professor with the University of Nice, Sophia-Antipolis, France, and at the University of York, U.K., respectively. He has served as an Associate Editor for the IEEE TRANSACTIONS ON SIGNAL PROCESSING (2002–2006 and since 2011), the IEEE SIGNAL PROCESSING LETTERS (2006–2010), the *Research Letters in Signal Processing* (2007–2009), the Hindawi *Journal of Electrical and Computer Engineering* (since 2009), the EURASIP *Signal Processing Journal* (since 2011), and as a Guest Editor for the EURASIP *Journal on Wireless Communications and Networking*. He has also served as an elected member of the Sensor Array and Multichannel (SAM) Technical Committee of the IEEE Signal Processing Society (since 2011), as the Technical Co-Chair of the IEEE International Symposiums on Personal Indoor and Mobile Radio Communications (PIMRC) 2005, Berlin, Germany, as the Technical Program Chair of the IEEE International Symposium on Wireless Communication Systems (ISWCS) 2010 in York, U.K., and as the General Chair of ISWCS 2013 in Ilmenau, Germany.